

**SEMMELWEIS EGYETEM
DOKTORI ISKOLA**

Ph.D. értekezések

3456.

FILIPOV TEODÓRA

**Diagnosztikus és terápiás radiológiai kutatások
című program**

Programvezető: Dr. Dósa Edit, egyetemi tanár

Témavezető: Dr. Deák Pál Ákos, klinikai főorvos

Ultrasound-Guided Minimally Invasive Diagnostic and Therapeutic Innovations in Interventional Radiology

Ph.D. Thesis

Teodora Filipov M.D.

Translational Medicine Program

Doctoral School of Theoretical and Translational Medicine

SEMMELWEIS UNIVERSITY



Supervisor:

Pál Ákos Deák M.D. Ph.D.

Official reviewers:

Ádám Zoltán Farkas M.D. Ph.D.

Bálint Botz M.D. Ph.D.

Head of the Complex Examination Committee:

Prof. Zsolt Molnár M.D. Ph.D.

Members of the Complex Examination Committee:

Andrea Párniczky M.D. Ph.D.

Zoltán Pál M.D. Ph.D.

Péter Fehérvári M.D. Ph.D.

Prof. Zoltán Németh M.D. Ph.D.

Budapest

2026

“The absurd is lucid reason noting its limits.”

— Albert Camus

TABLE OF CONTENTS

1. LIST OF ABBREVIATIONS	5
2. STUDENT PROFILE	6
2.1. Vision and mission statement, specific goals	6
2.2. Scientometrics.....	6
2.3. Future plans.....	6
3. SUMMARY OF THE THESIS	7
4. GRAPHICAL ABSTRACT	8
5. INTRODUCTION	9
5.1. Overview of the topic	9
5.2. Cryoablation.....	9
5.3. Shear Wave Elastography	10
6. OBJECTIVES	12
6.1. Study I. – Cryoablation for Fibroadenoma with Liquid Nitrogen Based System: a retrospective analysis of prospectively collected data	12
6.2. Study II. – Investigating the role of ultrasound-based shear wave elastography in kidney transplanted patients: Correlation of non-invasive fibrosis detection, kidney dysfunction and biopsy results. A systematic review and meta-analysis	12
7. METHODS	13
7.1. Study I.....	13
7.1.1. Study Design	13
7.1.2. Study Setting and Participants	13
7.1.3. Ethics and Patient Consent	13
7.1.4. Procedure	13
7.1.5. Variables and Outcome Measures	15
7.1.6. Statistical Methods and Evidence Synthesis	15
7.2. Study II	16

7.2.1.	Methodology and Protocol	16
7.2.1.	Information Sources, Search Strategy and Eligibility Criteria	16
7.2.2.	Study Selection and Data Extraction	16
7.2.3.	Quality of Evidence Assessment and Risk of Bias.....	17
7.2.4.	Data Synthesis and Analysis	17
8.	RESULTS.....	19
8.1.	Study I: Retrospective Analysis of Prospectively Collected Data.....	19
8.1.1.	Study Population	19
8.1.2.	Procedure	23
8.1.3.	Primary Outcome: Efficacy – Volume Reduction.....	24
8.1.4.	Efficacy – Volume Reduction Subgroup Analyses	25
8.1.5.	Secondary Outcome – Safety	27
8.2.	Study II: Meta-Analysis.....	28
8.2.1.	Study Search and Selection	28
8.2.2.	Basic Characteristics of Included Studies	29
8.2.3.	Quantitative and qualitative synthesis	34
8.2.3.1.	Correlation between elastography and biopsy results	34
8.2.3.2.	Correlation between elastography and arterial Resistive Index	35
8.2.3.3.	Correlation between elastography and creatinine	35
8.2.3.4.	Correlation between elastography and eGFR.....	36
8.2.4.	Risk of Bias Assessment	37
9.	DISCUSSION.....	46
9.1.	Summary of Findings, International Comparisons	46
9.1.1.	Study I	46
9.1.2.	Study II	47
9.1.3.	Shared Advantages and Clinical Impact.....	50

9.2. Strengths	52
9.2.1. Study I	52
9.2.2. Study II	52
9.3. Limitations	52
9.3.1. Study I	52
9.3.2. Study II	52
10. CONCLUSIONS.....	54
10.1. Study I	54
10.2. Study II.....	54
11. IMPLICATIONS FOR PRACTICE.....	55
12. IMPLICATIONS FOR RESEARCH	56
12.1. Methodology and Study Design.....	56
12.2. New Areas	56
13. IMPLICATIONS FOR POLICY MAKERS	57
14. FUTURE PERSPECTIVES	58
15. REFERENCES	59
16. BIBLIOGRAPHY.....	65
16.1. Publications Related to the Thesis	65
16.2. Publications not Related to the Thesis	65
17. ACKNOWLEDGEMENTS	66

1. LIST OF ABBREVIATIONS

BMI	Body mass index
CA	Cryoablation
CI	Confidence interval
eGFR	Estimated glomerular filtration rate
FA	Fibroadenoma
IF/TA	Interstitial fibrosis and tubular atrophy
IQR	Interquartile range
IR	Interventional radiology
Max	Maximum
Min	Minimum
MRE	Magnetic resonance elastography
N, n	Number of patients
r	Correlation coefficient
RI	Resistive index
SD	Standard deviation
SWE	Shear Wave Elastography
US	Ultrasound
U.S. FDA	United States Food and Drug Administration
VAE	Vacuum-assisted excision

2. STUDENT PROFILE

2.1. Vision and mission statement, specific goals

My vision is to reduce patient discomfort in hospital settings by advancing less invasive diagnostic tools and minimally invasive treatments in everyday clinical practice. My mission is to remain at the forefront of radiological interventions by researching innovative techniques, staying current with technological advancements, and applying image-guided procedures to enhance patient-centred care. My specific goals include conducting research on ultrasound-based ablation methods and techniques, as well as developing a high level of expertise in ultrasound diagnostics and ultrasound-guided interventional procedures.



2.2. Scientometrics

Number of all publications:	3
Cumulative IF:	9.5
Av IF/publication:	3.17
Ranking (SCImago):	D1:1, Q1:2
Number of publications related to the subject of the thesis:	2
Cumulative IF:	4.9
Av IF/publication:	2.45
Ranking (Sci Mago):	D1:-, Q1:2
Number of citations on MTMT (independent):	75
H-index:	2

The detailed bibliography of the student can be found on page 67.

2.3. Future plans

As a radiology resident passionate about interventional radiology, my future plans focus on advancing ultrasound-based, minimally invasive therapies to improve patient outcomes while reducing discomfort. I aim to combine technical expertise with evidence-based practice, precise patient selection, and clear communication, contributing to radiology's evolving role as a patient-centred, therapeutic speciality.

3. SUMMARY OF THE THESIS

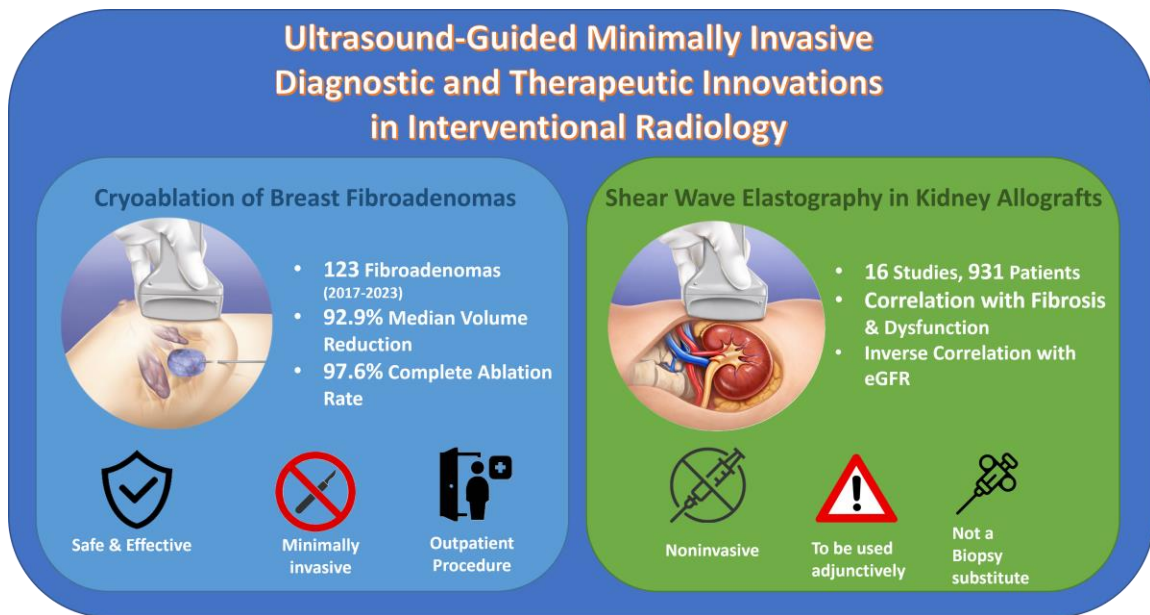
Interventional radiology (IR) has an increasingly important role in modern medicine by offering minimally invasive, image-guided diagnostic and therapeutic solutions that reduce patient burden while maintaining clinical efficacy. This thesis evaluated two ultrasound-based (US-based) applications that reflect these principles.

The first study is a retrospective analysis of prospectively collected data assessing liquid nitrogen-based cryoablation (CA) in patients with biopsy-proven breast fibroadenomas (Fas). Between 2017 and 2023, 78 patients with 123 FA were treated under real-time US guidance using local anesthesia. The primary objectives were to evaluate safety, efficacy, and the feasibility of cryoprobe relocation for treating large or multiple lesions in a single session. At 12 months, a median FA volume reduction of 92.9% was achieved, including lesions up to 80 mm in diameter. The complete treatment rate was 97.6%, and only one minor complication was observed. Treatment efficacy was consistent across patient age, body mass index, lesion size, and cryoprobe type. These findings support CA as a safe, effective, and cosmetically favorable outpatient alternative to surgical excision for FA.

The second study is a systematic review and meta-analysis investigating the correlation between US-based shear wave elastography (SWE) and renal allograft fibrosis and dysfunction. Sixteen observational studies involving 931 kidney transplant recipients were included. Pooled analyses demonstrated a moderate positive correlation between renal stiffness and biopsy-proven fibrosis, as well as correlations with resistive index (RI) and serum creatinine, and an inverse correlation with estimated glomerular filtration rate (eGFR). However, substantial heterogeneity and variable risk of bias limited the strength of these associations. While elastography reflects underlying structural and functional changes in renal allografts, current evidence does not support its use as a substitute for biopsy.

In conclusion, this thesis demonstrates the clinical value of US-based techniques across both therapeutic and diagnostic domains. CA offers an effective, minimally invasive treatment for benign breast disease, while SWE shows promise as an adjunctive, noninvasive tool for monitoring kidney transplant function. Together, these findings highlight the expanding role of IR in delivering patient-centered, image-guided care.

4. GRAPHICAL ABSTRACT



5. INTRODUCTION

5.1. Overview of the topic

IR has transformed patient care by using imaging modalities to guide therapy with minimal trauma. Modern IR procedures adhere to the guiding principle of “reducing trauma via minimally invasive access” to shorten recovery times and lower complication rates.(1)

In practice, US guided techniques exemplify this model: they provide real-time, radiation free visualization of instruments and targets, enabling precise therapy under local anesthesia. For example, percutaneous US-guided CA uses ultrasonic imaging to visualize the growing ice-ball during tumor freezing. By sparing healthy tissues and reducing procedural invasiveness, these approaches yield outcomes comparable to surgery with fewer complications and shorter hospital stays. Indeed, recent reviews emphasize that IR procedures improve quality of care and cost-effectiveness by enabling fast recovery and outpatient treatment for complex conditions.(1, 2)

5.2. Cryoablation

Breast FA represent the most common benign breast lesion, particularly in women under 30 years of age, and account for a large proportion of the approximately 1.3 million breast biopsies performed annually in Europe.(3, 4) Although benign, FAs frequently cause psychological distress due to concerns about malignancy, discomfort, and cosmetic issues.(5) Standard management includes observation or surgical excision, including vacuum-assisted excision (VAE); however, minimally invasive techniques such as thermal ablation have emerged as alternative treatment options.(6-9)

CA is the only thermal ablation technique utilizing cooling agents, such as liquid nitrogen, and is approved by both the United States Food and Drug Administration (U.S. FDA) and the European *conformité européenne* (CE) for the treatment of FAs.(9, 10)

CA is a minimally invasive thermal ablative technique that destroys tissue by rapid freezing by applying extreme cold, typically under image guidance. A cryoprobe inserted into the center of the target lesion induces formation of an expanding ice ball, within which temperatures progressively decrease toward the probe. Rapid cooling increases intracellular osmolarity and freezes extracellular water, leading to dehydration and

rupture of cells, while intracellular ice crystal formation during freezing and subsequent thawing phases further disrupts cellular membranes and organelles. Experimental data indicate that irreversible cell death generally occurs at temperatures between approximately -20°C and -40°C , with the -20°C isotherm commonly regarded as the minimum lethal threshold for most soft tissues. Additional injury results from microvascular damage, thrombosis, and ischemia during freeze–thaw cycles, which enhance the extent of necrosis and ensure complete ablation of the target lesion.(11, 12)

CA offers several advantages over surgery, including real-time US visualization of the ice ball, minimal scarring, use of local anesthesia, rapid recovery, and suitability for office-based procedures.(13) Previous studies have demonstrated CA to be a safe and effective treatment for both benign and malignant breast lesions, with favorable short- and long-term outcomes and high patient and physician satisfaction.(14, 15) The present study aimed to further support existing evidence regarding the effectiveness and safety of CA and to demonstrate the feasibility of cryoprobe relocation, which enables the treatment of large and/or multiple FAs in a single session through multiple treatment cycles.

5.3. Shear Wave Elastography

Renal allograft dysfunction commonly progresses to interstitial fibrosis and tubular atrophy (IF/TA), which represents the leading cause of kidney transplant failure.(16) IF/TA develops early after transplantation and arises from multiple factors, including acute or subclinical rejection and ischemia–reperfusion injury.(17) Clinically, it may manifest as elevated serum creatinine, reduced eGFR, proteinuria, and hypertension.(16, 18)

Monitoring graft function is essential, and kidney biopsy remains the diagnostic gold standard, providing critical information for clinical management.(19) However, biopsies are invasive and associated with risks such as hemorrhage, arteriovenous fistula, and, rarely, graft loss, and they are contraindicated in several clinical situations. Additionally, undergoing a biopsy represents significant psychological burden due to increased vulnerability, fear of the unknown and of procedural pain, as well as the requirement to remain bedridden for two hours after the procedure. Consequently, there is a growing interest in noninvasive alternatives.(20-25)

SWE is an advanced US technique that quantifies the elastic properties of tissue by generating and measuring the propagation of shear waves within that tissue. SWE uses focused acoustic radiation force pulses from the US transducer to induce localized tissue displacement, which creates shear waves that travel perpendicular to the primary US beam. These shear waves move much more slowly than conventional US waves, and their velocity is directly related to tissue stiffness: stiffer tissues allow faster shear-wave propagation, while softer tissues slow the waves. By tracking the shear-wave velocity at each location, SWE calculates the shear modulus and displays it in a color-coded elastogram overlaid on standard B-mode images, allowing quantitative measurement of elasticity in units such as meters per second or kilopascals. This quantitative stiffness mapping helps distinguish different tissue properties beyond conventional grayscale imaging and has proven useful in evaluating traumatic or pathologic conditions in a variety of soft tissues.(26)

US-based elastography has emerged as a promising tool, as tissue stiffness reflects underlying pathological changes.(27) SWE has proven utility in assessing liver fibrosis, with expanding applications to other organs, including the kidney.(28) However, kidney SWE measurements are influenced by several confounders such as anisotropy, perfusion, urinary pressure, hydronephrosis, and body mass index (BMI).(16) While some studies report a positive correlation between kidney stiffness and fibrosis,(24, 29) others show no significant association.(30, 31) In light of the controversy, we performed a meta-analysis to examine the relationship between SWE findings, biopsy results, and clinical parameters of renal dysfunction in kidney transplant recipients.

6. OBJECTIVES

6.1. Study I. – Cryoablation for Fibroadenoma with Liquid Nitrogen Based System: a retrospective analysis of prospectively collected data

Our retrospective analysis investigates the safety and therapeutic efficacy of liquid nitrogen-based CA in patients with single or multiple FAs, including those with large lesions. Furthermore, to demonstrate the feasibility of a cryoprobe relocation approach that enables treatment of large and/or multiple FAs in a single session using multiple treatment cycles.

6.2. Study II. – Investigating the role of ultrasound-based shear wave elastography in kidney transplanted patients: Correlation of non-invasive fibrosis detection, kidney dysfunction and biopsy results. A systematic review and meta-analysis

In our meta-analysis we aimed to analyse if SWE findings can be correlated to the many measures of kidney dysfunction, most importantly biopsy results. Other parameters assessed were various clinical renal dysfunction indicators, like the decrease of eGFR, increased serum creatinine and arterial RI. We hypothesized that change in tissue stiffness assessed by SWE can be correlated to the changes in these factors.

7. METHODS

7.1. Study I

7.1.1. Study Design

This retrospective, single-centre observational study aimed primarily to demonstrate the efficacy of CA for FA. The study was designed and reported in accordance with the Strengthening the Reporting of Observational Studies in Epidemiology (STROBE) guidelines to ensure clear and comprehensive reporting. A secondary objective was to assess the safety of CA for the treatment of FA overall, including its use with the cryoprobe relocation technique.

7.1.2. Study Setting and Participants

All procedures and data acquisition were conducted at Premier Med Healthcare, Training and Research Institute in Budapest, Hungary, a private centre that treats FAs using liquid nitrogen-based CA. All CA procedures performed at the centre between 2017 and 2023 were consecutively included, provided that the FA had been confirmed by core needle biopsy. Data were accessed for research purposes through June 1, 2024. The authors had access to information that could identify individual participants during and after data collection.

7.1.3. Ethics and Patient Consent

This study was approved by the local institutional ethics review board (License No. 70/2024). All procedures were conducted in accordance with the ethical standards of the institutional research committee and the principles of the 1964 Declaration of Helsinki and its subsequent amendments or comparable ethical standards. Written informed consent was obtained from all participants included in the study.

7.1.4. Procedure

All patients underwent CA based on personal preference and were deemed suitable candidates for the procedure. They presented to Premier Med Healthcare, Training, and Research Institute after declining surgical excision, which is the standard of care for FA patients in Hungary. CA procedures were performed under US guidance (Fig. 1) using the ProSense™ liquid nitrogen-based CA system and cryoprobes (IceCure Medical Ltd.,

Israel). Cryoprobes (FAP7800000, 2.4 mm, 13G, 134 mm, elliptic ice ball shape; FAP7100000, 3.4 mm, 10G, 127 mm, spherical ice ball shape; or FAP7200000, 3.4 mm, 10G, 140 mm, elliptic ice ball shape) and cycle durations were selected by the treating physician based on the size, number, accessibility, and anatomical location of the FA, in accordance with the manufacturer's user manual.(32)

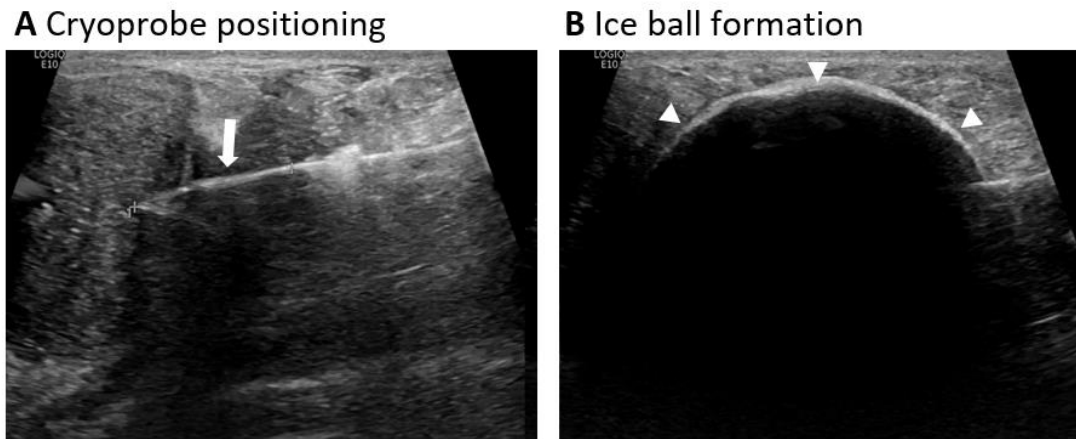


Figure 1. Procedure real-time images (Original images taken by the authors.)

US-guided cryoprobe (white arrow) centering within the FA (a) and subsequent ice ball (arrowheads) formation (b)

The 2.4 mm (13G) probe was primarily used for smaller FAs or in situations where a narrower diameter minimized tissue trauma during insertion. The 3.4 mm (10G) probes produced larger ice balls and were therefore suitable for medium to larger lesions. Variations in probe length (127 mm vs. 134–140 mm) enabled the physician to access lesions at different depths while ensuring accurate positioning of the cooling zone at the lesion centre. Additionally, the availability of spherical and elliptical ice-ball configurations allowed better adaptation to lesion geometry, facilitating complete coverage of the FA.

Freeze–thaw–freeze cycle durations were individualized to achieve full lesion coverage by the -20°C lethal isotherm of the ice ball, which was monitored in real time under US guidance. When the ice ball did not fully encompass the lesion, such as in larger FAs, the

cryoprobe was sequentially repositioned after each freeze–thaw–freeze cycle to ensure complete treatment.

All patients received local anaesthesia with 1% lidocaine (10 ml) prior to the procedure. When the FA was located within 1 cm of the skin, saline hydrodissection (10–50 ml) was performed to prevent skin frostbite. None of the patients underwent surgical excision following CA.

7.1.5. Variables and Outcome Measures

FA dimensions before and after CA were assessed using US imaging, and the volume was calculated as $[\pi/6 \times \text{length} \times \text{width} \times \text{diameter} (\text{cm}^3)]$. The duration of the CA freeze–thaw–freeze cycles and any complications occurring during the procedure or within 3 days post-CA were recorded. Follow-up visits were scheduled at 1, 3, 6, and 12 months.

7.1.6. Statistical Methods and Evidence Synthesis

For statistical analysis, two analysis sets were defined. The Safety Analysis Set (SAS) included all patients who underwent the CA procedure and captured adverse events occurring during the procedure and up to 3 hours post-procedure. The Analysis Set (AS) comprised all patients who underwent CA without major protocol deviations and had at least one follow-up visit at either 6 months (± 1.5 months) or 12 months (± 1.5 months) post-CA. Major protocol deviations included incomplete treatment, missing follow-up, or a follow-up duration of less than 1.5 months.

Continuous variables were summarized using the mean, standard deviation (SD), median, and range, while categorical variables were presented as counts and percentages. The proportion of procedure-related adverse events was reported with 95% confidence intervals (95% CI).

For each lesion and at each follow-up visit, the percentage reduction in lesion size relative to baseline was calculated. The statistical significance of lesion size reduction at the 6- and 12-month follow-up visits was assessed using the Wilcoxon signed-rank test.

Subgroup analyses were performed according to probe type using the Kruskal–Wallis test, and correlations with age and body mass index (BMI) were evaluated using

Spearman's rank correlation coefficient. A p-value < 0.05 was considered statistically significant for all analyses.

Statistical analyses and data management were conducted using SAS version 9.4 (SAS Institute Inc., Cary, NC, USA).

7.2. Study II

7.2.1. Methodology and Protocol

The study was reported in accordance with the PRISMA 2020 guidelines, with reference to the Cochrane Handbook for Systematic Reviews of Interventions.(33) The study protocol was registered in the PROSPERO database under registration number CRD42021283152.

7.2.1. Information Sources, Search Strategy and Eligibility Criteria

A systematic literature search was conducted on October 17, 2021, across three major medical databases (MEDLINE, Embase, and CENTRAL). The search was repeated on February 15, 2023, to identify any additional relevant studies. No language or date restrictions were applied. The same search strategy was used in all databases: “(kidney OR renal) AND (transplant OR graft OR recipients OR allograft) AND (elasticity OR elastograph* OR "shear-wave" OR "shear wave" OR SWE OR ultrasonograph* OR ultrasound OR acoustic OR ARFI) AND (dysfunction OR stiffness OR fibrosis OR structure OR parenchyma)”.

Observational studies involving kidney transplant recipients that reported correlation coefficients between SWE values and parameters of kidney dysfunction were considered eligible. Kidney dysfunction parameters included fibrosis, RI, serum creatinine, and eGFR. Animal studies, reviews, letters, case reports, and studies employing transient or magnetic resonance elastography (MRE) were excluded.

7.2.2. Study Selection and Data Extraction

Two independent reviewers (TF and ASz) screened potentially eligible studies. EndNote X9 (Clarivate Analytics) reference management software was used during the study selection process. Following the removal of duplicates, studies were screened by title and abstract, after which full-text articles were assessed for eligibility. Inter-rater agreement

was evaluated using Cohen's kappa coefficient (κ) after each screening step. Any disagreements regarding study eligibility were resolved by consultation with a third reviewer (BT). Backward and forward citation searching of all eligible articles was also performed to identify additional relevant studies.

Data extraction was conducted independently by two authors (TF and AF), with disagreements resolved by a third reviewer (BT). Data were collected using predefined Excel spreadsheets (Microsoft Corporation). Extracted information included study characteristics (first author, year of publication, Digital Object Identifier [DOI], study design, study location, and number of patients), baseline patient characteristics (age, sex, time since transplantation, donor type [living or deceased], and Banff fibrosis scores, when available), and technical details of the US devices and SWE techniques. Raw SWE data, available information on operators, and outcome data were also collected. For study outcomes, correlation coefficients (Pearson's or Spearman's) and corresponding p values between SWE measurements and kidney dysfunction parameters were extracted or calculated. When key data were missing, study authors were contacted for clarification.

7.2.3. Quality of Evidence Assessment and Risk of Bias

Risk of bias was assessed independently by two authors (FT and AF) using the QUADAS-2 tool,(34) which evaluates both risk of bias and concerns regarding applicability. Risk of bias was examined across four domains: patient selection, index test, reference standard, and flow and timing. Applicability concerns were assessed in three domains: patient selection, index test, and reference standard. Any disagreements in quality assessment were resolved with the involvement of a third reviewer (BT).

Assessment of publication bias was not performed, as the number of included studies did not reach the minimum threshold of 10 required for this analysis.

7.2.4. Data Synthesis and Analysis

A minimum of three studies per outcome was required for inclusion in the meta-analysis. Outcomes that did not meet this criterion were presented in Forest plots for descriptive visualization only. Statistical analyses were performed using the R programming language (R Core Team, 2019; version 4.1). Random-effects meta-analyses of correlation data were conducted using the *metacor* function from the meta package (version 5.5).(35)

Using the extracted correlation coefficients (r) from individual studies, pooled correlation coefficients with 95% CI were calculated employing a random-effects model with inverse-variance weighting and Restricted Maximum Likelihood method estimator for between-study variance.(36) Prior to analysis, correlation coefficients were transformed to Fisher's z values ($z = 0.5 \log_e (1+r/1-r)$), except in studies with very large sample sizes.(37) This transformation was performed automatically by the *metacor* function by setting the *sm* argument to "ZCOR".

Pearson's and Spearman's correlation coefficients were analyzed separately and not pooled together, as Pearson's correlation assumes a linear relationship between continuous variables, whereas Spearman's rank correlation assesses monotonic but potentially nonlinear associations. Correlation strength was interpreted as follows: 0.00–0.10 negligible, 0.10–0.39 weak, 0.40–0.69 moderate, 0.70–0.89 strong, and 0.90–1.00 very strong.(38) A p value < 0.05 was considered statistically significant. Forest plots were used to visually summarize the results.

Statistical heterogeneity was assessed using Cochran's Q test, with $p < 0.10$ indicating significant heterogeneity. The I^2 statistic and its 95% CI were also reported, representing the proportion of total variation across studies attributable to between-study heterogeneity.(39) In accordance with the Cochrane Handbook for Systematic Reviews of Interventions,(33) I^2 values of 0%–40% were considered potentially unimportant, 30%–60% moderate, 50%–90% substantial, and 75%–100% considerable heterogeneity. Where applicable, prediction intervals were also reported to indicate the expected range of effects in future studies.(40)

8. RESULTS

8.1. Study I: Retrospective Analysis of Prospectively Collected Data

8.1.1. Study Population

In total, 78 patients with 123 FAs underwent CA procedures. Cases in which a palpable lump was detected after treatment were followed and monitored regularly. None of these lesions showed growth, and consequently, no patients required surgical excision following CA. The patient flow is illustrated in Figure 2.

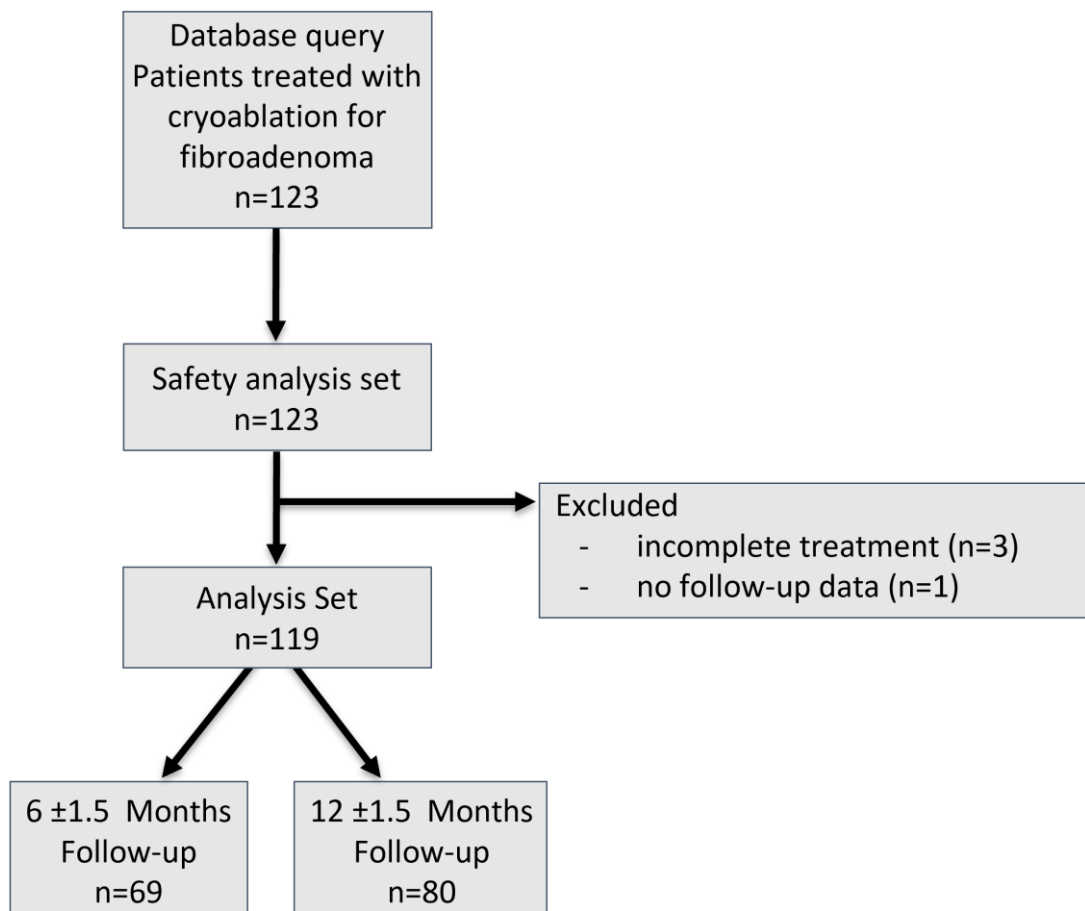


Figure 2. Patient's flow (*n* number of fibroadenomas)

The mean and median ages of the patients were 34.2 years (SD \pm 9.8) and 31.5 years (IQR 26–34), respectively, with an age range of 17 to 66 years. The majority of patients (62%) were 35 years old or younger. The mean body mass index (BMI) was 22.3 ± 4.5 , and most women (81.7%) had a BMI below 25 (Table 1).

Table 1. Patient characteristics

Parameter		SAS	AS
Age (years)	N	78	76
	Mean \pm SD	34.2 \pm 9.8	34.3 \pm 9.9
	Min, Max	17, 66	17, 66
	Median [IQR]	31.5 [26, 43]	32.5 [26, 43]
Weight (kg)	N	60	58
	Mean \pm SD	61.8 \pm 10.7	61.7 \pm 10.8
	Min, Max	42, 100	42, 100
	Median [IQR]	61 [54, 66]	61 [54, 66]
BMI	N	60	58
	Mean \pm SD	22.3 \pm 4.5	22.3 \pm 4.5
	Min, Max	16, 37.8	16, 37.8
	Median [IQR]	21.9 [19.1, 23.9]	21.8 [19.1, 23.9]
BMI <25	N	49	47
	%	81.7	81.0

SAS Safety Analysis Set; *AS* Analysis Set; *N* number of patients with available data; *SD* standard deviation; *Min* minimum; *Max* maximum; *IQR* interquartile range; *kg* kilogram; *BMI* body mass index;

The number of FAs per patient ranged from 1 to 4. Most patients (85%) had one or two FAs, with 60% presenting with a single lesion and 25% with two lesions (Table 2).

Table 2. Number of FAs per patient

Number of FAs	Number of Patients (%)	Total Number of FAs
1	47 (60)	47
2	19 (25)	38
3	10 (13)	30
4	2 (3)	8
Total	78	123

FA fibroadenoma

FAs were evenly distributed between the left and right breasts, with the upper outer quadrant being the most common location (28%) (Figure 3).

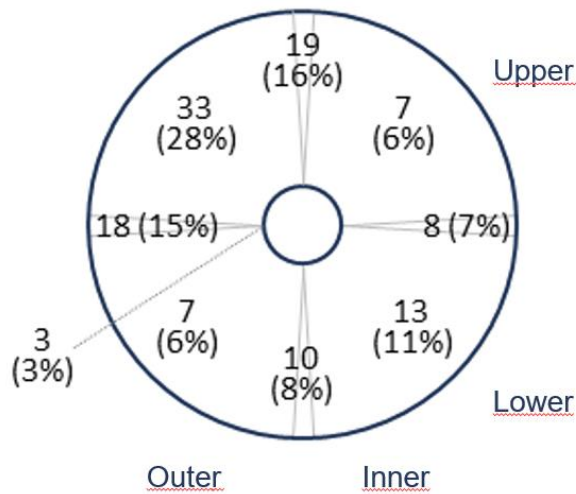


Figure 3. Fibroadenoma localisation

Distribution of the different FAs by quadrant location.

FAs' size, assessed by the maximum lesion diameter, and volume showed wide variability. Diameters ranged from 7 mm to 80 mm (mean 25.0 ± 10.8), while volumes ranged from 0.1 to 62.8 cm³ (mean $5.7 \text{ cm}^3 \pm 7.9 \text{ cm}^3$).

In the majority of procedures (90.2%), a 3.4 mm (10G) cryoprobe was used, in accordance with the manufacturer's recommendations (see Methods section for details). The mean procedure time for the freeze–thaw–freeze cycle was 13.0 ± 10.4 minutes (Table 3).

Table 3. FA characteristics at baseline and procedure features

Parameter			SAS	AS
			N=122	N=119
FA				
FA size	Width	Mean \pm SD	25 \pm 10.9	24.8 \pm 10.7
	(mm)	Min, Max	7, 80	7, 80
		Median [IQR]	25 [16, 32]	25 [16, 31]
Height		Mean \pm SD	19.7 \pm 8.6	19.6 \pm 8.6
	(mm)	Min, Max	6, 50	6, 50
		Median [IQR]	19.5 [13, 25]	19.0 [13, 25]
Depth		Mean \pm SD	14.2 \pm 7.4	13.8 \pm 6.5
	(mm)	Min, Max	3, 54	3, 38
		Median [IQR]	13 [9, 18]	13 [9, 18]
Volume		Mean \pm SD	5.7 \pm 8.0	5.4 \pm 7.5
	(cm ³)	Min, Max	0.1, 62.8	0.1, 62.8
		Median [IQR]	3.5 [0.9, 7.4]	3.3 [0.9, 7.2]
FA location		Left breast	59 (48.4%)	58 (48.7%)
		Right breast	63 (51.6%)	61 (51.3%)

Parameter	SAS		AS	
	N=122		N=119	
Procedure				
Cryoprobe diameter		2.4 (13G)	12 (9.8%)	12 (10.1%)
	(mm)	3.4 (10G)	110 (90.2%)	107 (89.9%)
Probe length		127 (10G)	70 (57.4%)	68 (57.1%)
	(mm)	134 (13G)	12 (9.8%)	12 (10.1%)
		140 (10G)	40 (32.8%)	36 (32.8%)
Cryoablation time		N	116 ¹	112 ¹
	(minute)	Mean ± SD	13.0 ± 10.4	12.8 ± 9.9
		Min, Max	3.3, 56	3.3, 56
		Median [IQR]	9 [6, 15]	9 [6, 15]
Follow up time		N	123	119
	(months)	Mean ± SD	16.3 ± 10.0	16.2 ± 10.0
		Min, Max	1.1, 42.2	1.1, 42.2
		Median [IQR]	13.0 [11.7, 23.3]	12.9 [11.7, 23.3]

¹ For 5 subjects, the cryoablation procedure was done on two FAs during the same procedure. Therefore, the procedure time for these cases was only considered once.

SAS Safety Analysis Set; *AS* Analysis Set; *N* number of patients; *SD* standard deviation; *IQR* interquartile range; *Min* minimum; *Max* maximum; *kg* kilogram; *cm* centimeter

8.1.2. Procedure

In most cases (76%, 91/119), a single freeze-thaw-freeze cycle was used per FA. The same approach was applied more than one lesion was present, provided the lesions were located close to each other (≤ 5 mm apart). In the remaining cases, one or more cryoprobe relocations were performed by partially or completely withdrawing and repositioning the

probe to allow additional freeze–thaw–freeze cycles. Probe relocation was employed when 1) two or more FAs were located far apart, 2) the FA was large, or 3) the lesion’s location did not permit complete treatment within a single cycle.

8.1.3. Primary Outcome: Efficacy – Volume Reduction

At the 12-month follow-up (mean 16.3 ± 10 months), patients with available data demonstrated a significant median reduction in FA volume of 92.9% (IQR 73.6–100; $p < 0.0001$). Volume reduction occurred gradually over time, with a pronounced decrease observed at the 6-month follow-up (median 80.6% [IQR 56.6–92.6]) followed by a more modest reduction between 6 and 12 months (Figure 4). Analyses included all treated FAs regardless of initial size, encompassing lesions with maximum diameters of up to 80 mm and volumes as large as 62.8 cm³.

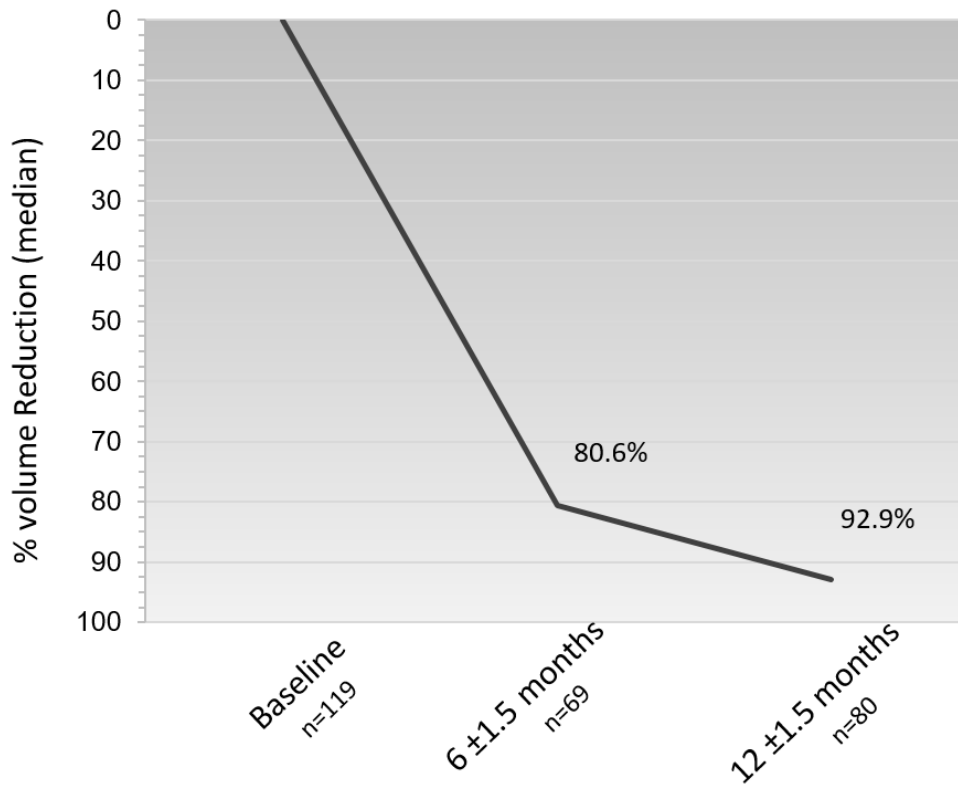


Figure 4. Median percent FA volume reduction.

The median percentage volume reduction of FA at 6 ± 1.5 and 12 ± 1.5 months was calculated for all FAs that had data at either time point (see Methods for details).

8.1.4. Efficacy – Volume Reduction Subgroup Analyses

Subgroup analyses were conducted to assess whether patient-, lesion-, or procedure-related characteristics influenced the percentage of FA volume reduction at 12 months. Variables evaluated included age, body mass index (BMI), lesion size (>4 cm), and cryoprobe type. None of these factors showed a statistically significant association with treatment response, indicating that the efficacy of CA was consistent across different patient characteristics, lesion sizes, and cryoprobe types.

Spearman's correlation analyses for age and BMI were not statistically significant ($p = 0.69$ and $p = 0.46$, respectively). Similarly, the Kruskal–Wallis test demonstrated no significant difference in 12-month volume reduction among the three cryoprobe types used ($p = 0.6831$).

Seven patients presented with large FAs (>4 cm in the largest dimension), accounting for a total of eight lesions. Patient ages ranged from 17 to 45 years, and lesion sizes ranged from 41 to 80 mm. Three patients (P1, P3, and P6) each had a single lesion larger than 4 cm; one patient (P2) had two lesions larger than 40 mm; and three patients (P4, P5, and P7) had one large lesion along with two additional lesions smaller than 40 mm (Table 4). As observed for smaller lesions, the volumes of large FAs decreased over time following CA, with an initial marked reduction followed by a more gradual decrease during extended follow-up (Figure 5). At a mean follow-up of 12.9 ± 4.6 months (range 3.2–17.7 months), the mean and median volume reduction rates were $87 \pm 1\%$ and 91% (IQR 82%–91%), respectively. One lesion (L3) in patient 5 (P5) demonstrated a rapid linear reduction, reaching an 84% volume decrease at 3.2 months; however, this patient was subsequently lost to follow-up, and the final reduction could not be determined.

Table 4. Characteristics of patients with a lesion(s) larger than 40 mm

Patient (P) number	Age (Years)	Number of lesions	Lesion (L) number and size* (mm)	Lesion Location	Number of cycles	Total Cryoablation time (minute)
P1	26	1	L1, 45	UOQ	2	15
P2	17	2	L1, 42	9:00	3	56
			L2, 44	9:00	3	
P3	45	1	L1, 80	UOQ	3	24
P4	42	3	L1 22	9:00	1	51
			L2, 32	6:00	1	
			L3, 41	12:00	1	
P5	38	3	L1, 16	LIQ	1	36
			L2, 28	6:00	1	
			L3, 42	LIQ	1	
P6	30	1	T1, 48	UIQ	3	33
P7	34	3	T1, 21	LOQ	1	48
			T2, 21	9:00	1	
			T3, 43	9:00	1	

UOQ Upper Outer quadrant; *UIQ* Upper Inner Quadrant; *LOQ* Lower Outer Quadrant; *LIQ* Lower Inner Quadrant; *mm* millimeter

* In the largest dimension

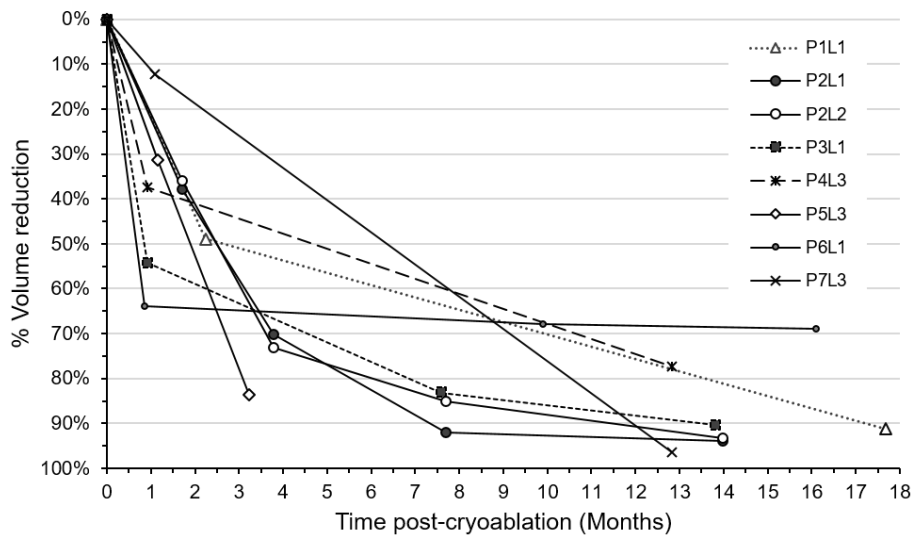


Figure 5. Volume reduction for lesions larger than 40 mm

The graph presents the percentage volume reduction over time following CA of eight FAs in seven patients. Each line represents an individual FA with available follow-up measurements. Volume reduction was calculated at each time point where post-procedural data were available (see Methods for more details).

8.1.5. Secondary Outcome – Safety

One adverse event was reported (1/123=0.81% [95%CI: 0.02%-4.45%]), consisting of a minor skin burn that resolved with conservative management using warming pads, without the need for further intervention.

Three incomplete treatments were documented (3/125, 2.4%). One was due to a technical limitation (cryoprobe malfunction), which resulted in an untreated peripheral zone of approximately 2 mm. Another was related to the lesion’s proximity to the nipple, leaving a 1 mm peripheral zone untreated. The third involved a patient who had previously undergone CA for two FAs; at the 1-year follow-up, residual viable (vascularized) tissue was detected on US in the medial (12 × 23 mm) and caudolateral (13 × 7 mm) regions, prompting a second CA procedure to complete treatment. Consequently, the overall complete treatment rate was 97.6% (122/125).

8.2. Study II: Meta-Analysis

8.2.1. Study Search and Selection

The systematic search identified a total of 6,956 records. Inter-rater reliability was high, with Cohen's kappa values of 0.82 for title and abstract screening and 1.00 for full-text selection. Following the study selection process, 16 studies (24, 29, 41-54) were included in the meta-analysis, including one study (41) identified through reference searching. A detailed overview of the study selection process is presented in Figure 6.

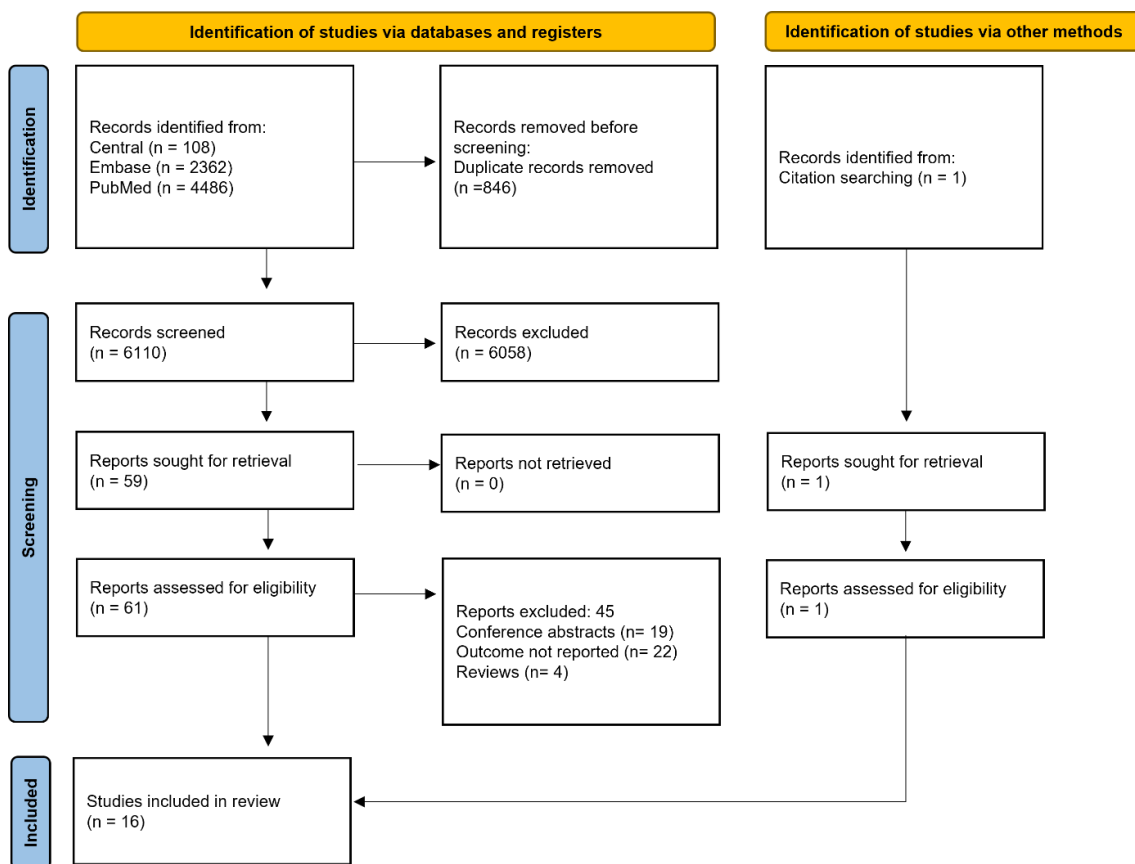


Figure 6. PRISMA 2020 flowchart representing the study selection process.(55)

8.2.2. Basic Characteristics of Included Studies

Baseline characteristics of the study populations and technical features of the included studies are summarized in Tables 5 and 6, respectively. The articles were published between 2010 and 2022, and a total of 931 patients were included in the meta-analysis. One study (45) focused on a pediatric population, while all others evaluated adult participants. Overall, the studies included patients from nine different countries. Two articles (48, 54) were published in languages other than English and were translated with the assistance of a professional translator.

Study populations were heterogeneous with respect to age (range: 4 months to 79 years), sex distribution (15%–49.2% female), and kidney function. Inclusion criteria varied across studies but were generally based on the assessment of renal transplant recipients using US. Some studies enrolled patients with suspected graft pathology, whereas others included stable recipients or a combination of both.

Table 5. Main characteristics of included studies

Study	Correlation coefficient	Study period	Country	No. of patients	Age (year)		Sex (Female, %)	Donor living/ deceased	Time elapsed since Tx (m) mean (range)	Mean creatinine (mg/dl)	Mean eGFR
					Mean \pm SD	Range					
Agrawal et al. 2021	Pearson's	10.2018-07.2020	India	40	39.2 \pm 11.7	21-61	15	N/A	22 (12-26)	N/A	63.3
Barsoum et al. 2022	Spearman's	02.2021-08.2021	Egypt	36	N/A	N/A	N/A	36/0	4,33 (2-8)	2,76	N/A
Chhajer et al. 2021	Pearson's	01.2017-03.2019	India	172	43.8	9-64	26.1	N/A	23.9 (3-180)	N/A	N/A
Chiocchini et al. 2017	Spearman's	N/A	Italy	41	52 \pm 16	N/A	38.1	1/40	9 ^a (1-288)	3.6	24.9
Dai et al. 2014	Spearman's	10.2010-07.2013	China	54	38 \pm 10	20-65	N/A	N/A	N/A	N/A	N/A
Desvignes et al. 2021	Spearman's	N/A	France	26	N/A	4m-18y	38.5	N/A	N/A	N/A	N/A
Grenier et.al. 2012	Pearson's	01.2010-05.2010	France	39	51 ^a	18.5-69.9	51	47/2	26.6 ^a (0.3-214.3)	1.9	34
Ghonge et al. 2018	Pearson's	10.2014-3.2016	India	60	40.8 \pm 11.3	20-73	15	60/0	26.8 (0.3-160)	0.76/1.9/3.9 ^b	83.1/47.7/31.3 ^b

He et al. 2014	Spearman's	12.2011-03.2013	China	102	38 ±12	18-64	32.3	N/A	31 (1-120)	N/A	N/A
Järv et al. 2019	Spearman's	03.2017-11.2017	Estonia	100	53.3 ±9.4	22-79	41	N/A	N/A	N/A	53.8
Quin et al. 2022	Pearson's & Spearman's	09.2020-08.2021	China	43	43 ^a	38-56	11.6	7/36	48 ^a (28-64)	2.35 ^a	31.2
Soudmand et al. 2018	Pearson's	N/A	Turkey	65	38.8 ±14	24.8-52.8	23.1	51/14	N/A	2.4	N/A
Stock et al. 2010	Spearman's	03.2009-06.2009	Germany	18	54.3 ±14.6	26-76	27.8	2/16	22 ^a (4.4-54.3)	2.6	28
Tukhbatullin et al. 2017	Pearson's	02.2015-05.2017	Russia	32	42.9 ±2.4	N/A	N/A	N/A	N/A	N/A	N/A
Wang et al. 2017	Pearson's	N/A	Taiwan	40	45.3	21-68	35	27/13	N/A	3.9	27.6
Yang et al. 2022	Spearman's	03.2021-11.2021	China	63	45 ^a	32-52	49.2	N/A	38 ^a (12-90)	2,4 ^a	N/A

^a: parameters represented as median, ^b: stable group/acute dysfunction group/chronic dysfunction group

eGFR estimated glomerular filtration rate, *m* months, *mg/dl* milligrams/deciliter, *N/A* not available, *SD* standard deviation, *Tx* transplantation

Table 6. Technical attributes of elastography in included studies

Study	Operators		Technical attributes			ROI		Elastography evaluation	
	N o.	Experience (y)	Device	Manufacturer	Transducer	Renal compartment	Location	Technique	U
Agrawal et al. 2021	N/A	N/A	iU22	Philips Healthcare	C5-1 convex (5-1 MHz)	N/A	upper, middle, lower pole	SWE	kPa
Barsoum et al. 2022	N/A	N/A	Aplio 500	TOSHIBA	6C1 curvilinear (B-mode)/ 14L5 linear (SWE)	N/A	N/A	SWE	kPa
Chhajer et al. 2021	N/A	N/A	Logiq E9	GE Healthcare	N/A	N/A	upper, middle, lower pole	SWE	kPa
Chiocchini et al. 2017	2	5	iU22	Philips Healthcare	C5-1 convex	N/A	middle third	SWE	kPa
Dai et al. 2014	N/A	N/A	Acuson S2000	Siemens Healthineers	4C1 convex (2-4 MHz)	cortex	upper, middle, lower pole	p-SWE	m/s
Desvignes et al. 2021	4	7-25	Aixplorer®	SuperSonic Imagine	convex low frequency (2–5MHz)	cortex	lower pole	2D-SWE	kPa
Grenier et.al. 2012	2	N/A	Aixplorer®	SuperSonic Imagine	SC6-1 convex (3.5 MHz)	cortex and medulla	N/A	2D-SWE	kPa

Ghonge et al. 2018	1	15	EPIQ-7G	Philips Healthcare	C5-1 convex	N/A	upper, lower, midinterpolar	p-SWE	kPa
He et al. 2014	2	N/A	Acuson S2000	Siemens Healthineers	4C1 curved linear array (1,75-4MHz)	N/A	middle third	p-SWE	m/s
Järv et al. 2019	2	>20	Affiniti 70	Philips Healthcare	C5-1 convex (5-1 MHz)	cortex	upper, lower pole	SWE	kPa
Quin et al. 2022	1	>10	MyLab 8Exp	Esaote SpA	C1-8 convex	cortex	N/A	P-SWE	kPa
Soudmand et al. 2018	1	N/A	Acuson S2000	Siemens Healthineers	6C1 curvilinear	cortex	N/A	p-SWE	m/s
Stock et al. 2010	3	N/A	Acuson S2000	Siemens Healthineers	curved array (4-1 MHz)	N/A	upper, middle, lower pole	p-SWE	m/s
Tukhbatullin et al. 2017	N/A	N/A	Aixplorer®	SuperSonic Imagine	convex (1-6 MHz)	N/A	upper, lower pole	2D-SWE	kPa
Wang et al. 2017	1	N/A	Acuson S3000	Siemens Healthineers	linear (4-9 MHz)	cortex	N/A	p-SWE	m/s
Yang et al. 2022	N/A	N/A	Voluson E20	GE Healthcare	C6-1 curvilinear (B-mode)/ L2-9 linear (SWE)	cortex	N/A	SWE	kPa

kPa kilopascal, *MHz* megahertz, *m/s* millimeters/second, *N/A* not available, *p-SWE* point-shear wave elastography, *SWE* shear wave elastography, *y* year

8.2.3. Quantitative and qualitative synthesis

8.2.3.1. Correlation between elastography and biopsy results

Nine studies (24, 29, 42-45, 47, 50, 51), comprising a total of 494 patients, reported correlation coefficients between stiffness measured by SWE and histopathologically assessed fibrosis (Figure 7). Pooled analyses demonstrated a moderate positive correlation for Pearson ($r=0.48$; CI: 0.20, 0.69) and Spearman correlation coefficients ($r=0.57$; CI: 0.35, 0.72). Heterogeneity analyses indicated marked heterogeneity among the studies with I^2 values of 84% ($p = 0.002$) and 74% ($p= 0.002$) for Pearson and Spearman correlations, respectively.

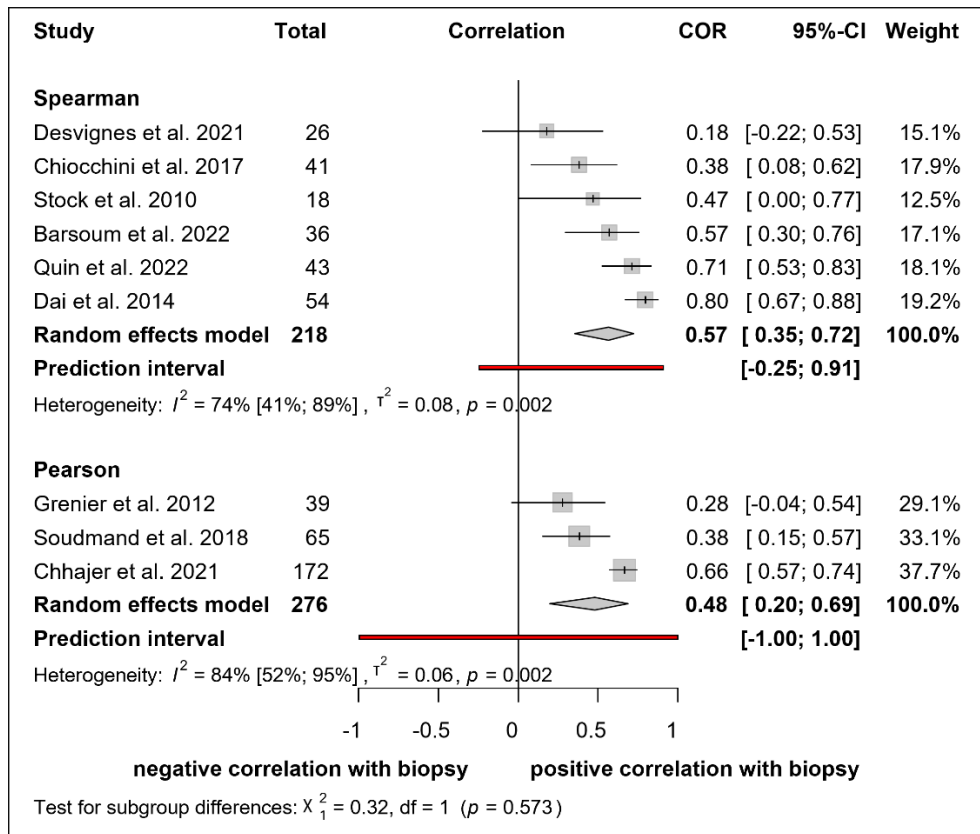


Figure 7. Forest plot representing a moderate positive correlation between elastography and biopsy results

8.2.3.2. Correlation between elastography and arterial Resistive Index

Eight studies (24, 41, 43, 46, 50, 51, 53, 54), including a total of 371 patients, evaluated the association between SWE measurements and renal arterial RI (Figure 8). Pooled Pearson's correlation between SWE and RI demonstrated a weak positive association ($r=0.37$; CI: 0.12, 0.57), with substantial heterogeneity among studies ($I^2=73\%$; $p < 0.011$). In contrast, pooled Spearman correlation for the same outcome showed no significant association ($r= -0.02$; CI: -0.24 to 0.20) and low heterogeneity ($I^2=17\%$; $p=0.302$)

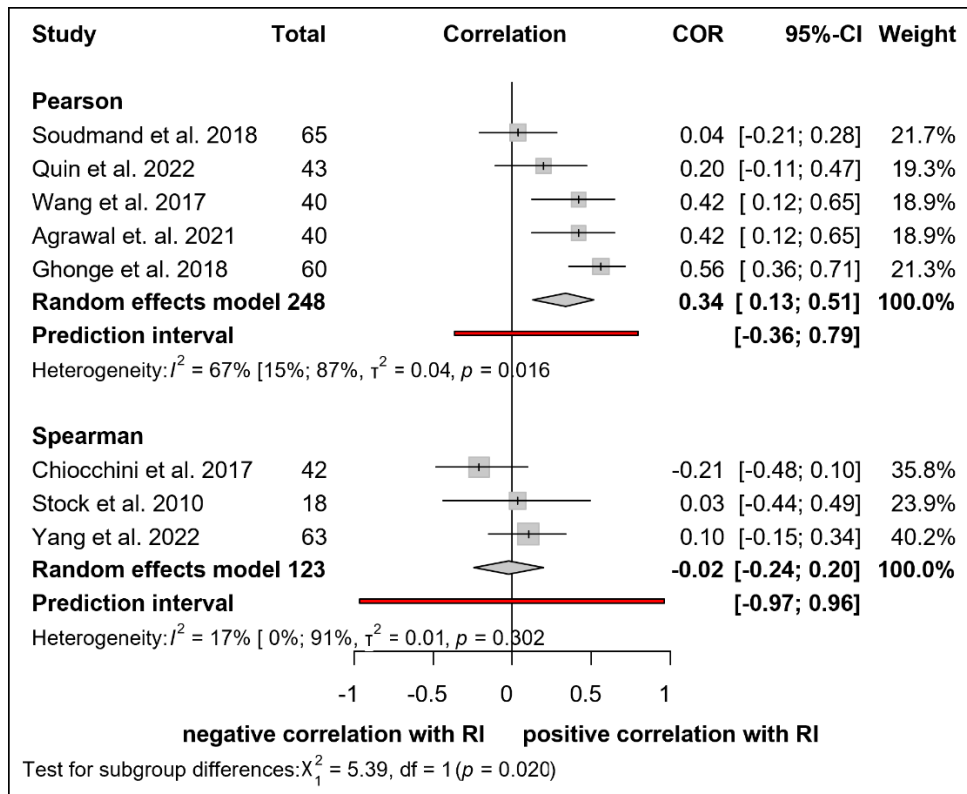


Figure 8. Forest plot representing a weak positive correlation between RI and elastography

8.2.3.3. Correlation between elastography and creatinine

The association between SWE measurements and serum creatinine levels was examined in nine studies (24, 29, 41, 43, 46, 49, 50, 52, 54), encompassing a total of 478 patients (Figure 9). Our results show a moderate positive Pearson's correlation between these two

parameters ($r=0.50$; CI: 0.1, 0.72), with considerable heterogeneity among studies ($I^2=73\%$; $p < 0.001$). Pooled results for Spearman's correlation showed negligible correlation ($r=0.10$; CI: -0.04 to 0.23), with no observed heterogeneity ($I^2=0\%$; $p=0.953$).

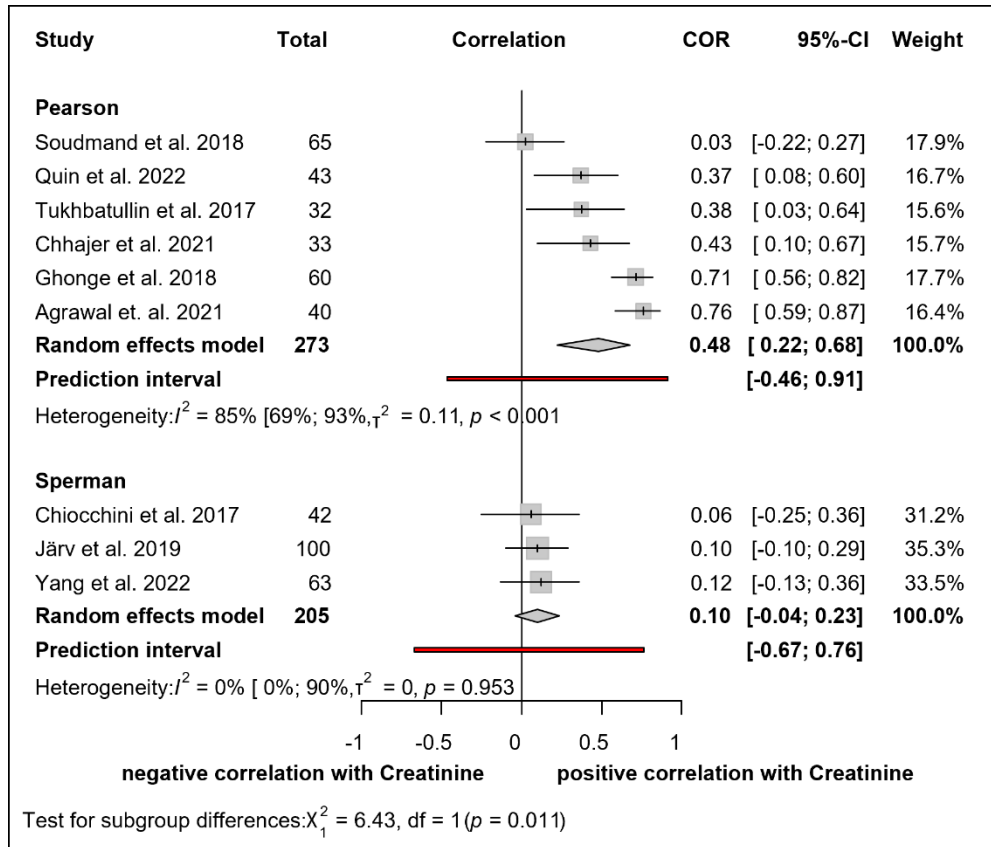


Figure 9. Forest plot representing a moderate positive correlation between creatinine and elastography

8.2.3.4. Correlation between elastography and eGFR

For eGFR six studies (41, 43, 46, 48-50) reported correlation coefficients, comprising a total of 380 patients (Figure 10). The pooled Pearson correlation demonstrated a moderate negative association between SWE and eGFR ($r = -0.65$; CI: -0.81 to 0.40). In this case, heterogeneity was substantial ($I^2=73\%$, $p=0.023$). The results with pooled Spearman's correlation coefficient did not show a statistically significant correlation ($r = -0.24$; CI: -0.66 to 0.30), and heterogeneity between the studies was significant ($I^2=95\%$; $p < 0.001$).

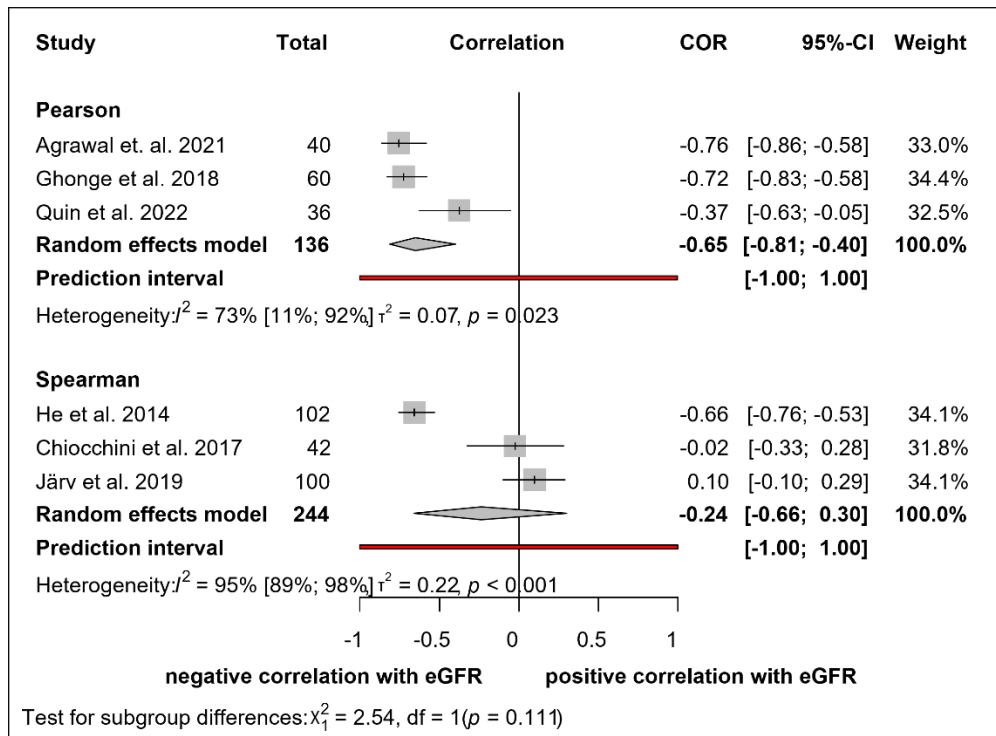


Figure 10. Forest plot representing no correlation between eGFR and elastography

8.2.4. Risk of Bias Assessment

Among the four studies (43-45, 51) that evaluated the correlation between SWE and histopathology using Spearman's correlation, only two (44, 51) did not report whether the index test and reference standard were interpreted blindly. Regarding RI, concerns about bias were high in the domains of index test and reference standard, as SWE and Doppler US were examinations performed in the same session by the same radiologist, precluding blinded interpretation. However, one study (46) reported that US examinations were conducted blinded to clinical data. Consequently, the overall risk of bias for this outcome was considered high, although concerns regarding applicability were deemed low.

Assessment of outcomes related to laboratory parameters was more challenging because detailed laboratory test results were often not reported. Nevertheless, most studies (29, 43, 46, 48, 49) stated that SWE assessments were performed blinded to clinical data.

Overall, the risk of bias varied from low to high across different outcomes, while concerns regarding applicability were consistently judged to be low (Table 6-13, Figure 10-17).

Table 6. Assessment of the risk of bias and applicability of included studies for Spearman's correlation between elastography and biopsy results representing a low risk of bias with some uncertainty and no applicability concerns

STUDY	RISK OF BIAS				APPLICABILITY CONCERNS		
	Patient selection	Index test	Reference standard	Flow and timing	Patient selection	Index test	Reference standard
Desvignes et al. 2021	😊	😊	😊	😊	😊	😊	😊
Chiocchini et al. 2017	😊	😊	😊	😊	😊	😊	😊
Stock et al. 2010	😊	😊	?	😊	😊	😊	😊
Barsoum et al. 2022	😊	?	?	😊	😊	😊	😊
Quin et al. 2022	😊	😊	😊	😊	😊	😊	😊
Dai et al. 2014	😊	?	?	?	😊	😊	😊

😊 Low Risk 😞 High Risk ? Unclear Risk

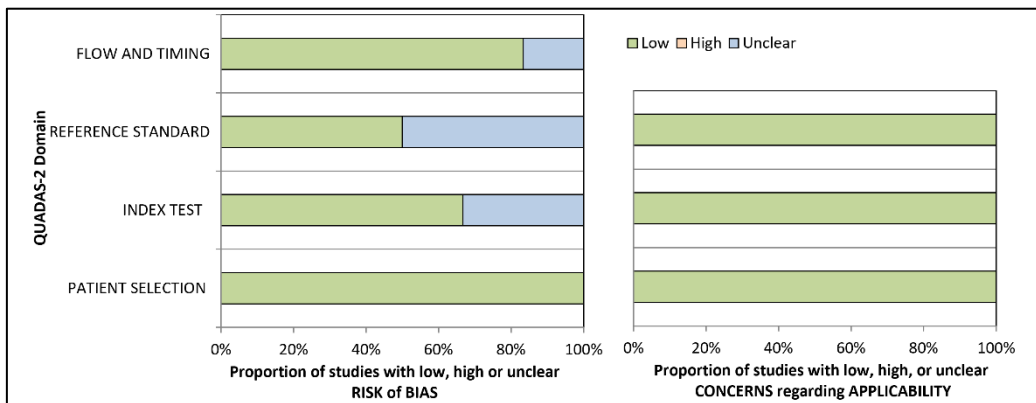


Figure 10. Diagram representing a low risk of bias with some uncertainty and no applicability concerns of included studies for the correlation between elastography and biopsy results assessed by Spearman's correlation

Table 7. Assessment of the risk of bias and applicability of included studies for Pearson's correlation between elastography and biopsy results showing low risk

STUDY	RISK OF BIAS				APPLICABILITY CONCERNS		
	Patient selection	Index test	Reference standard	Flow and timing	Patient selection	Index test	Reference standard
Gernier et.al. 2012	😊	😊	😊	😊	😊	😊	😊
Soudmand et al. 2018	😊	😊	😊	😊	😊	😊	😊
Chhajer et al. 2021	😊	😊	😊	😊	😊	😊	😊

😊 Low Risk 😞 High Risk ? Unclear Risk

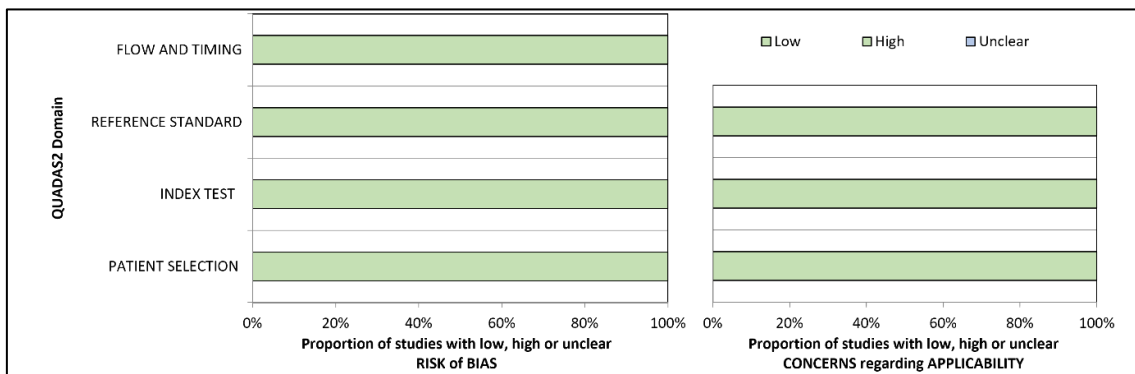


Figure 11. Diagram representing a low risk of bias and applicability of included studies for the correlation between elastography and biopsy results assessed by Pearson's correlation

Table 8. Assessment of the risk of bias and applicability of included studies for Pearson's correlation between elastography and RI representing a high risk of bias in "reference standard" and "index test" domains and no applicability concerns

STUDY	RISK OF BIAS				APPLICABILITY CONCERNS		
	Patient selection	Index test	Reference standard	Flow and timing	Patient selection	Index test	Reference standard
Soudmand et al. 2018	😊	😞	😞	😊	😊	😊	😊
Quin et al. 2022	😊	😞	😞	😊	😊	😊	😊
Wang et al. 2017	😊	😞	😞	😊	😊	😊	😊
Agrawal et.al. 2021	😊	😞	😞	😊	😊	😊	😊
Ghonge et al. 2018	😊	😞	😞	😊	😊	😊	😊

😊 Low Risk 😞 High Risk ? Unclear Risk

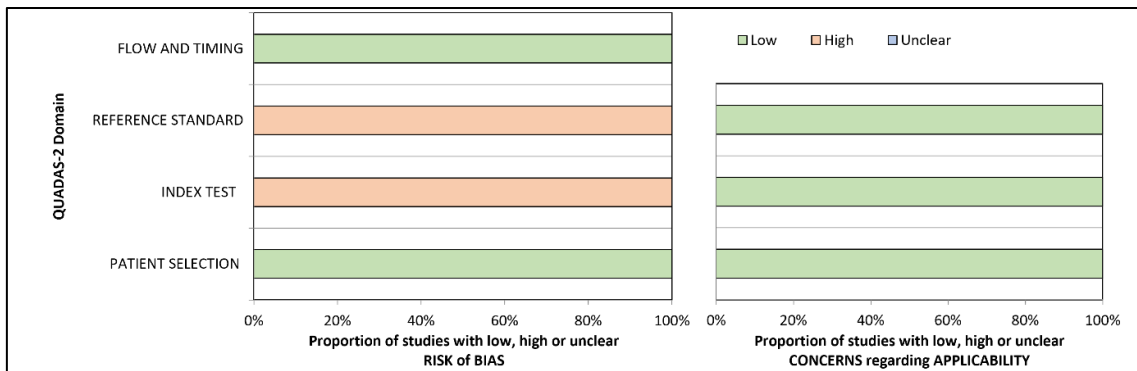


Figure 12. Diagram representing a high risk of bias in "reference standard" and "index test" domains and no applicability concerns of included studies for the correlation between elastography and RI assessed by Pearson's correlation

Table 9. Assessment of the risk of bias and applicability of included studies for Spearman's correlation between elastography and RI representing a high risk of bias in "reference standard" and "index test" domains and no applicability concerns

STUDY	RISK OF BIAS				APPLICABILITY CONCERNS		
	Patient selection	Index test	Reference standard	Flow and timing	Patient selection	Index test	Reference standard
Chiocchini et al. 2017	😊	😞	😞	😊	😊	😊	😊
Stock et al. 2010	😊	😞	😞	😊	😊	😊	😊
Yang et al. 2022	😊	😞	😞	😊	😊	😊	😊

😊 Low Risk 😞 High Risk ? Unclear Risk

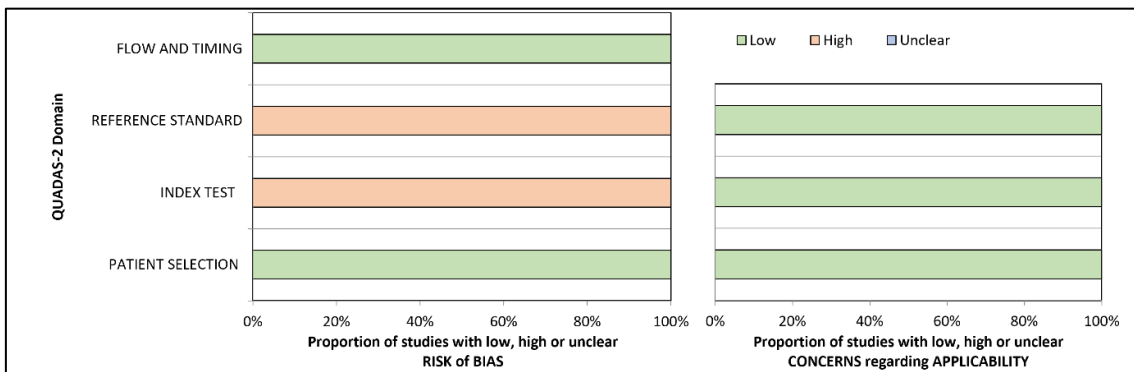


Figure 13. Diagram representing a high risk of bias in "reference standard" and "index test" domains and no applicability concerns of included studies for the correlation between elastography and RI assessed by Spearman's correlation

Table 10. Assessment of the risk of bias and applicability of included studies for Pearson's correlation between elastography and creatinine representing an uncertain risk of bias in "reference standard" and "index test" domains and no applicability concerns

STUDY	RISK OF BIAS				APPLICABILITY CONCERNS		
	Patient selection	Index test	Reference standard	Flow and timing	Patient selection	Index test	Reference standard
Soudmand et al. 2018	😊	?	?	😊	😊	😊	😊
Quin et al. 2022	😊	?	?	😊	😊	😊	😊
Tukhbatullin et al. 2017	😊	?	?	😊	😊	😊	😊
Chhajer et al. 2021	😊	😊	?	😊	😊	😊	😊
Ghonge et al. 2018	😊	😊	?	😊	😊	😊	😊
Agrawal et.al. 2021	😊	?	?	😊	😊	😊	😊

😊 Low Risk 😞 High Risk ? Unclear Risk

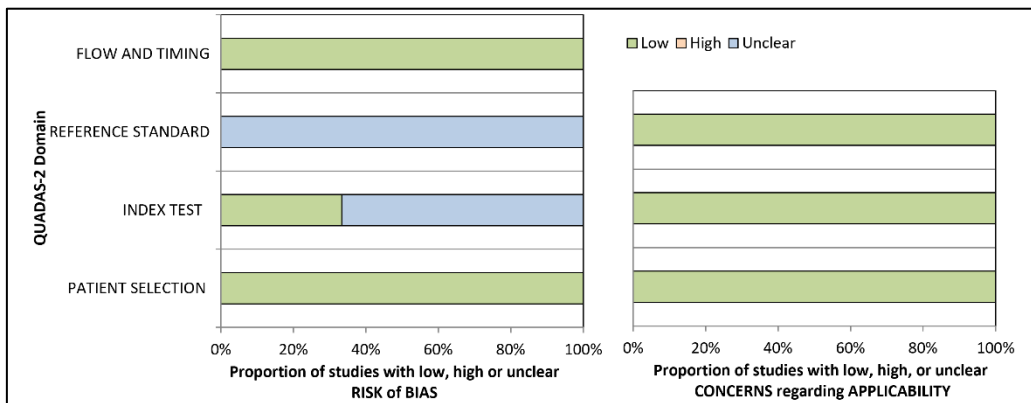


Figure 14. Diagram representing an uncertain risk of bias in "reference standard" and "index test" domains and no applicability concerns of included studies for the correlation between elastography and creatinine assessed by Pearson's correlation

Table 11. Assessment of the risk of bias and applicability of included studies for Spearman's correlation between elastography and creatinine representing an uncertain risk of bias in "reference standard" domain and no applicability concerns

STUDY	RISK OF BIAS				APPLICABILITY CONCERNS		
	Patient selection	Index test	Reference standard	Flow and timing	Patient selection	Index test	Reference standard
Chiocchini et al. 2017	😊	😊	?	😊	😊	😊	😊
Järv et al. 2019	😊	😊	?	😊	😊	😊	😊
Yang et al. 2022	😊	?	?	😊	😊	😊	😊

😊 Low Risk 😞 High Risk ? Unclear Risk

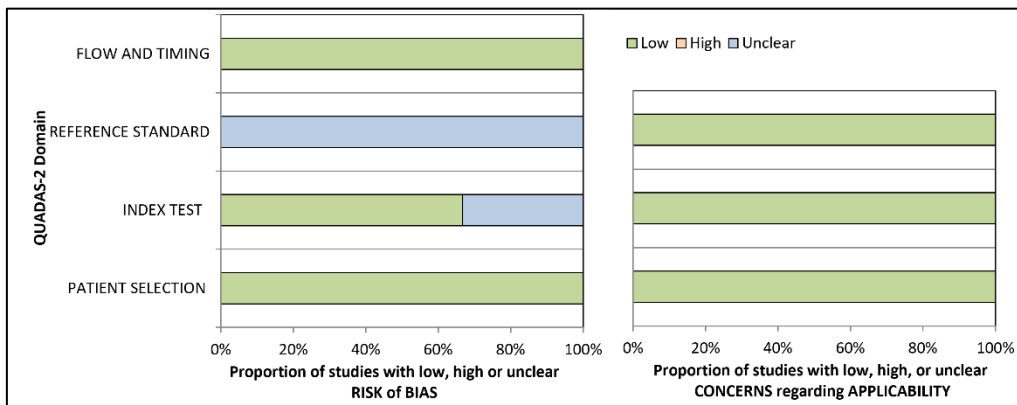


Figure 15. Diagram representing an uncertain risk of bias in "reference standard" and domain and no applicability concerns of included studies for the correlation between elastography and creatinine assessed by Spearman's correlation

Table 12. Assessment of the risk of bias and applicability of included studies for Pearson's correlation between elastography and eGFR representing an uncertain risk of bias in "reference standard" and "index test" domain and no applicability concerns

STUDY	RISK OF BIAS				APPLICABILITY CONCERNS		
	Patient selection	Index test	Reference standard	Flow and timing	Patient selection	Index test	Reference standard
Agrawal et al. 2021	😊	?	?	😊	😊	😊	😊
Chiocchini et al. 2017	😊	😊	?	😊	😊	😊	😊
Quin et al. 2022	😊	?	?	😊	😊	😊	😊

😊 Low Risk 😞 High Risk ? Unclear Risk

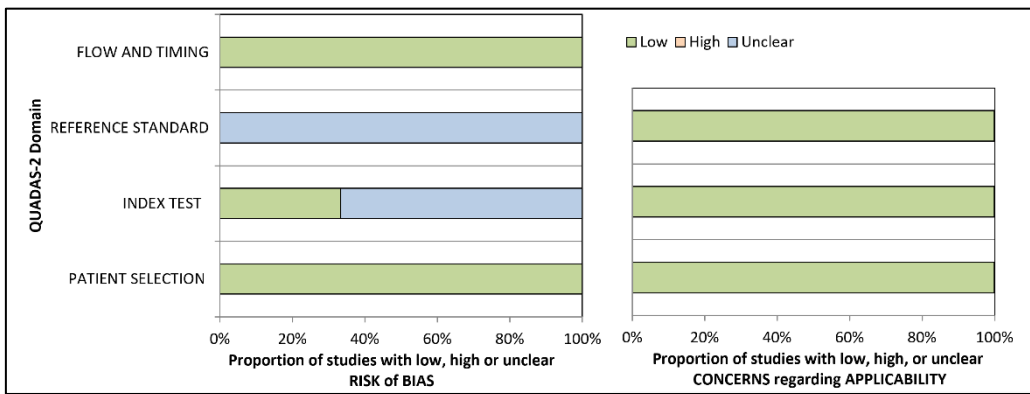


Figure 16. Diagram representing an uncertain risk of bias in "reference standard" and "index test" domain and no applicability concerns of included studies for the correlation between elastography and eGFR assessed by Pearson's correlation

Table 13. Assessment of the risk of bias and applicability of included studies for Spearman's correlation between elastography and eGFR representing an uncertain risk of bias in "reference standard" domain and no applicability concerns

STUDY	RISK OF BIAS				APPLICABILITY CONCERNS		
	Patient selection	Index test	Reference standard	Flow and timing	Patient selection	Index test	Reference standard
He et al. 2014	😊	😊	?	😊	😊	😊	😊
Chiocchini et al. 2017	😊	😊	?	😊	😊	😊	😊
Järv et al. 2019	😊	😊	?	😊	😊	😊	😊

😊 Low Risk 😞 High Risk ? Unclear Risk

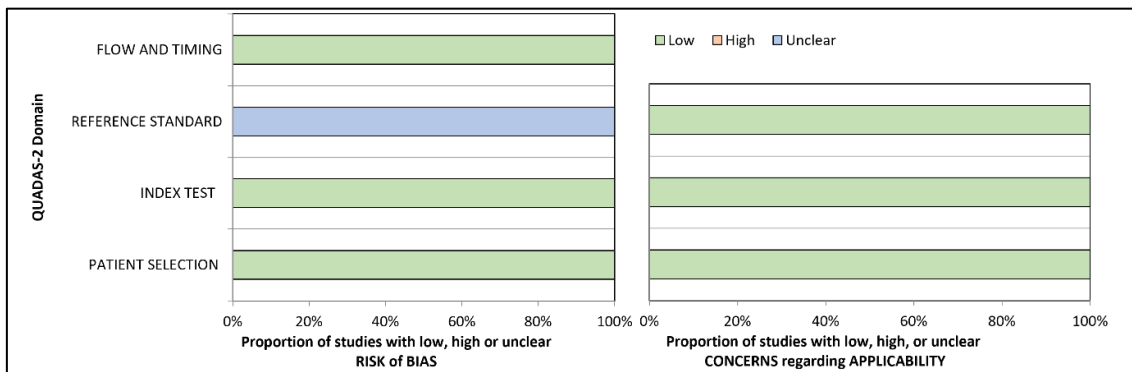


Figure 17. Diagram representing an uncertain risk of bias in "reference standard" domain and no applicability concerns of included studies for the correlation between elastography and eGFR assessed by Spearman's correlation

9. DISCUSSION

9.1. Summary of Findings, International Comparisons

9.1.1. Study I

This retrospective, single-center study represents the first Hungarian experience with CA for breast FA and evaluated treatment outcomes in a heterogeneous population with respect to age, lesion number, and FA size. CA was performed under local anesthesia, required a short procedural time, and allowed same-day discharge with immediate return to normal activities. Despite the use of multiple cryoprobe relocations in some cases, the complication rate was extremely low, with only one minor adverse event reported, comparing favorably with complication rates reported for VAE and surgical excision.(56-58)

Aesthetic outcomes were uniformly excellent, with no unfavorable cosmetic changes observed, and the complete treatment rate (97.6%) was comparable to or exceeded rates reported after VAE.(58) Treatment efficacy was high, with a median FA volume reduction of approximately 93% at 12 months, including lesions up to 80 mm in maximal diameter. No significant associations were found between volume reduction and patient age, body mass index, or cryoprobe type, suggesting a consistent treatment response across subgroups.

Compared with earlier studies reporting lower response rates in larger lesions,(6, 14, 15) the present study demonstrated volume reductions at 6 and 12 months that were equal to or greater than those previously published. Variability among studies is likely attributable to differences in lesion size, assessment methods, CA protocols, and follow-up duration.(15) The individualized treatment approach applied in this study—tailoring freeze cycles, probe relocation, and ice-ball coverage through multidisciplinary planning—likely contributed to the high efficacy observed.

Breast size, FA location, and breast tissue composition significantly affect the technical success and safety of CA. Maintaining a safe distance from the skin and chest wall is essential to avoid frostbite.(59, 60) Although FAs near the nipple can be technically challenging due to risks to nipple function and sensation, CA can be performed safely in this location. Dense breast tissue may further complicate cryoprobe positioning.(61)

Treatment may be recommended for patients with symptomatic FAs, such as those associated with pain, palpability, or growth, and includes hormone therapy, surgical excision (including VAE), and US-guided CA. The American Society of Breast Surgeons (October 2018) guidelines report that CA has comparable efficacy and safety to open surgical excision and endorse its use for FAs measuring less than 4 cm in maximum diameter.(9) CA offers cosmetic advantages for breast tumors, including FAs and breast cancer, as it preserves surrounding normal breast tissue and allows restoration of normal or near-normal breast appearance. Consistent with the present study, recent reports of CA for breast cancer show 100% patient satisfaction(62-64), compared with lower satisfaction rates following VAE.(58) Moreover, CA is a significantly shorter procedure (mean 13.0 ± 10.4 minutes per cycle in our study) and can be performed in an office setting under local rather than general anesthesia,(64, 65) which is particularly beneficial for women with multiple FAs.(6) Finally, CA is more cost-effective than surgical excision, with substantially lower procedural costs(14).

US-based volumetric follow-up was considered an appropriate surrogate for treatment success in biopsy-proven benign FAs.(8, 66) Given the predictable involution of treated lesions and their confirmed benign nature, post-treatment excision was neither clinically nor ethically justified. Overall, these findings support CA as a safe, effective, cosmetically favorable, and cost-efficient alternative to surgical management for breast FAs.

9.1.2. Study II

This systematic review and meta-analysis assessed the association between renal allograft stiffness measured by SWE, histopathological fibrosis, and clinical dysfunction parameters in kidney transplant recipients. Overall, the analysis demonstrated a positive correlation between SWE-measured kidney stiffness and biopsy-proven fibrosis, as well as positive correlations with RI and serum creatinine, and a negative correlation with eGFR.

SWE is already well established in the assessment of liver fibrosis,(67-71) and its application in renal allografts is technically advantageous due to the superficial pelvic location of transplanted kidneys.(72) Several studies have reported moderate-to-high diagnostic performance of SWE in identifying graft dysfunction and differentiating

fibrosis grades, with sensitivities and specificities ranging from approximately 70% to over 90%.(29, 41, 48) Compared with MRE, US-based SWE offers faster, more accessible, and cost-effective evaluation.(73-75)

IF/TA is a progressive process leading to declining kidney function and represents a major cause of allograft injury, with generally poor graft survival once chronic tubulointerstitial damage is established.(76, 77) The process begins early after transplantation, when histological changes precede functional impairment, and progresses rapidly during the first post-transplant year under the influence of immunologic factors, ultimately causing irreversible glomerulosclerosis and nephron loss.(17, 78) Currently, fibrosis assessment relies on biopsy, an invasive method that samples only a small fraction of the kidney.(76) Moreover, interpretation is limited by the semi-quantitative Banff classification, which is subject to variability and interobserver disagreement.(16, 79, 80)

Across the included studies, correlations between SWE and fibrosis varied widely, likely reflecting differences in patient populations, fibrosis severity, biopsy indications, and timing post-transplantation. Stronger correlations tended to be observed in cohorts with a higher prevalence of advanced fibrosis, suggesting that SWE may be more sensitive in detecting moderate-to-severe disease.(29, 43, 45, 47, 50, 51)

The relationship between SWE and Doppler-derived RI remains complex. RI reflects both vascular and parenchymal factors and is influenced by numerous systemic variables.(81-88) Although a moderate positive correlation between SWE and RI was identified, substantial heterogeneity across studies suggests these parameters may reflect overlapping but not identical pathophysiological processes.

Regarding laboratory markers, kidney stiffness correlated positively with serum creatinine and inversely with eGFR. However, since creatinine rises only in later stages of graft dysfunction,(89) these parameters are limited in detecting early IF/TA. Overall, while IF/TA has strong prognostic significance, conventional clinical markers alone cannot reliably predict their presence, supporting SWE as a potentially valuable adjunctive, noninvasive tool for allograft monitoring.

Since our publication interest is growing in applying SWE to monitor kidney allograft health, with several studies focusing on prognostic value, fibrosis assessment, and correlation with clinical parameters. A large prospective cohort (2020–2023) showed that

increased allograft stiffness measured by SWE—especially medullary stiffness >10 kPa—is associated with higher risk of adverse outcomes such as a decline in kidney function. Incorporating SWE parameters into machine-learning models (e.g., XGBoost) improved prediction of graft deterioration compared with conventional labs alone.(90) A prospective observational study by Ruidas et al. found that SWE parenchymal stiffness correlated with histopathological grades of IF/TA in chronic renal allograft injury, suggesting SWE may distinguish between mild, moderate, and severe graft fibrosis.(91) SWE medullary stiffness has been repeatedly shown to add incremental prognostic value for adverse outcomes in transplant recipients beyond traditional measures like eGFR and albumin, supporting its potential role in risk stratification.(92) Technical and variability issues (e.g., measurement heterogeneity, anisotropy effects, and operator dependence) continue to be noted, underlining the need for standardized protocols and larger multicenter studies to validate SWE as a reliable noninvasive biomarker in transplant care.(93)

9.1.3. Shared Advantages and Clinical Impact

Both US-guided CA and SWE illustrate the shared principles of modern image-guided interventions:

- Real-time US guidance allows continuous monitoring of instruments and treatment effects. During CA the growing ice-ball is directly seen, ensuring complete ablation margin.(2) Similarly, SWE provides instantaneous stiffness maps to guide diagnosis. Crucially, US involves no radiation, making repeated use safe.
- Reduced patient burden: These techniques avoid major surgery. CA is percutaneous and often outpatient, sparing patients large incisions, general anesthesia, and lengthy recovery.(1, 13) SWE entirely avoids any puncture, eliminating risks of bleeding or infection. In both cases, recovery is faster and discomfort is minimal.
- Safety and cost-effectiveness: By minimizing complications, these methods cut costs and improve value. IR procedures like CA have been shown to lower hospital days and complication rates relative to surgery.(2) SWE also reduces costs by limiting invasive tests. Overall, IR techniques are safer, faster, and more cost-effective for patients.(1, 13)
- Diagnostic and therapeutic roles: Together, they span IR's dual mission. CA provides a targeted therapy under imaging control, whereas SWE offers a diagnostic biomarker from imaging. Both leverage US's versatility: for example, SWE can noninvasively track response to therapy (e.g. measuring residual stiffness post-ablation) and help select patients for intervention.(13, 94)
- Alignment with current practice: In recent years these US-based methods have been integrated into guidelines and practice algorithms. Major societies now endorse US elastography for liver disease assessment (94) and increasingly for breast, thyroid, and musculoskeletal imaging. Similarly, CA's strong results have placed it in treatment guidelines for renal and other tumors.(2, 95) These trends reflect radiology's move toward image-guided, minimally invasive care and precision diagnostics.(96)

In summary, US based techniques like CA and SWE exemplify the value IR brings to modern medicine. They combine precision imaging with minimal invasiveness, yielding high-quality care with less morbidity. Recent literature strongly supports their expanding role in clinical practice.(2, 95) As IR continues to innovate, such approaches underscore

the specialty's impact: improving patient outcomes by making diagnosis and therapy safer, faster, and more patient centric.(1, 13)

9.2. Strengths

9.2.1. Study I

Our retrospective study represents one of the largest reported cohorts from the Central European region. A key strength is the demonstration that cryoprobe relocation—an approach that has been infrequently described in the literature—can be performed safely and effectively, particularly in the treatment of larger or multiple FAs. Furthermore, the study cohort was heterogeneous with respect to patient age, as well as the number and size of FAs, thereby reflecting the diversity encountered in routine clinical practice and enhancing the real-world relevance of the findings.

9.2.2. Study II

The systematic review and meta-analysis presented in this thesis is the first to evaluate the correlation between SWE and parameters of kidney dysfunction. The use of a rigorous and transparent methodology enabled a comprehensive assessment of renal function in a kidney transplant population, thereby strengthening the validity of the findings.

9.3. Limitations

9.3.1. Study I

Some limitations should also be acknowledged. This was a single-centre study without a control group, which limits the ability to draw comparative conclusions. In addition, the study population consisted exclusively of patients who preferred to undergo CA, which may introduce selection bias and limit the generalisability of the results to all patients with FAs. Finally, the retrospective study design resulted in incomplete capture of certain variables, such as palpation findings, which are inherently subjective and difficult to standardize.

9.3.2. Study II

Considering our work's limitations, only a limited number of studies were eligible for inclusion in the meta-analysis, and the study populations were heterogeneous. A more detailed exploration of heterogeneity was not feasible due to insufficient reporting of relevant variables, which precluded meaningful subgroup analyses. In particular,

subgroup analyses according to different grades of fibrosis could not be performed, as such data were not consistently reported in the included studies.

Transplanted kidneys are located in the iliac fossa, and therefore lie more superficially than native kidneys, allowing higher-quality SWE imaging.(48, 72, 97) Despite this technical advantage, further research is required to determine the sensitivity and specificity of SWE for detecting fibrosis in transplanted kidneys. In addition, the relationship between renal elasticity and clinical dysfunction parameters, including RI, serum creatinine, and eGFR, warrants further investigation to establish the reliability of SWE as an adjunctive tool in renal function assessment. Future studies should also report detailed population characteristics to facilitate more robust analyses.

10. CONCLUSIONS

10.1. Study I

In summary, this study provides further evidence that CA using a liquid nitrogen system is a safe and effective treatment modality for biopsy-proven breast FAs, resulting in a 92.9% reduction in lesion volume at one year following treatment. The findings suggest that the indications for CA may extend beyond traditionally selected patients to include those with larger lesions and multiple FAs. Importantly, the data demonstrate that multiple sequential probe repositionings can be performed without compromising procedural safety or therapeutic efficacy. CA was well tolerated, minimally invasive, and associated with rapid post-procedural recovery, supporting its feasibility as an outpatient alternative to surgical excision. By presenting real-world data from a heterogeneous patient population, this work contributes to the growing body of evidence supporting the broader clinical application of CA in the management of benign breast disease. However, despite these encouraging results, further prospective, controlled studies are warranted to confirm these findings and to more clearly define the role of CA within contemporary treatment paradigms.

10.2. Study II

In conclusion, this study demonstrated a moderate positive correlation between renal stiffness measured by SWE and histopathological findings on biopsy. The ability to noninvasively assess renal fibrosis following transplantation is of substantial clinical importance. Nevertheless, the current body of evidence remains insufficient to support the use of elastography as an alternative to biopsy in the longitudinal management and follow-up of kidney transplant recipients.

11. IMPLICATIONS FOR PRACTICE

The findings of this work support the broader clinical integration of minimally invasive, US-based diagnostic and therapeutic techniques. In kidney transplant care SWE shows potential as a complementary, noninvasive tool for assessing renal allograft fibrosis and dysfunction, particularly in patients where biopsy is contraindicated or repeated sampling is undesirable. While SWE cannot yet replace biopsy, its use may help guide clinical decision-making, risk stratification, and follow-up strategies when interpreted alongside conventional clinical and laboratory parameters.

For benign breast disease, CA using a liquid nitrogen-based system represents a safe, effective, and patient-centered alternative to surgical excision. Its minimal invasiveness, favorable cosmetic outcomes, rapid recovery, and suitability for outpatient settings support its broader adoption in appropriately selected patients. The demonstrated feasibility of treating larger and multiple FA in a single session further expands its practical applicability when performed by experienced interventional radiologists.

12. IMPLICATIONS FOR RESEARCH

12.1. Methodology and Study Design

Future research should focus on the development of standardized, vendor-specific SWE acquisition protocols to improve reproducibility and comparability across studies and clinical settings. Particular attention should be given to optimizing US parameters for renal tissue, addressing known confounders such as anisotropy, perfusion, and patient-related factors. Large, prospective studies correlating SWE findings with histopathology are needed to define clinically meaningful cut-off values for fibrosis grading and stages of allograft dysfunction.

In the context of CA, further prospective and multicenter studies with larger cohorts and standardized outcome reporting would strengthen the evidence base. While randomized comparisons with surgical techniques may be challenging due to fundamental differences in invasiveness and patient preference, well-designed comparative effectiveness studies could provide valuable insights into long-term outcomes, cost-effectiveness, and patient-reported measures.

12.2. New Areas

Emerging research should explore the integration of SWE with multiparametric US approaches, combining elasticity measurements with Doppler indices, contrast-enhanced US, and artificial intelligence–based image analysis to enhance diagnostic accuracy in renal transplantation. Longitudinal SWE monitoring may also help identify early, subclinical graft injury before irreversible damage occurs.

For interventional oncology and benign disease management, innovation should focus on refining image-guided ablation strategies, including real-time treatment monitoring, probe optimization, and personalized treatment planning. Expanding the use of CA to additional benign and selected malignant indications may further reduce reliance on surgery and advance the role of IR as a cornerstone of minimally invasive patient care.

13. IMPLICATIONS FOR POLICY MAKERS

Although CA is an accepted and U.S. FDA–approved treatment for benign breast lesions, specifically core-needle biopsy–confirmed FAs, it is not currently reimbursed by the National Health Insurance Fund of Hungary, nor widely funded across Europe.(10) It is anticipated that the efficacy and safety data presented in this study will contribute to the growing body of evidence supporting CA and help facilitate its future inclusion within national health insurance funds.

14. FUTURE PERSPECTIVES

The findings of this thesis reinforce the evolving role of radiology from a primarily diagnostic discipline toward a patient-centered, minimally invasive clinical specialty. As a radiology resident with a strong interest in IR, this work has further shaped my professional perspective on how imaging-guided therapies and advanced US techniques can directly improve patient outcomes while minimizing physical and psychological burden.

On a broader level, both CA and SWE exemplify the direction in which radiology is heading: toward precision medicine, reduced invasiveness, and closer patient interaction. As an aspiring interventional radiologist, my goal is to contribute to this transition by combining technical excellence with thoughtful patient selection, clear communication, and evidence-based practice. Future advances in US-based interventions will not only expand therapeutic possibilities but also place radiologists in a more active clinical role—one that allows us to offer patients treatments that are not only effective, but also safer, gentler, and more aligned with their individual needs and values.

15. REFERENCES

1. Campbell WAt, Chick JFB, Shin DS, Makary MS. Value of interventional radiology and their contributions to modern medical systems. *Front Radiol.* 2024;4:1403761.
2. Seager M, Kumar S, Lim E, Munneke G, Bandula S, Walkden M. Renal cryoablation - a practical guide for interventional radiologists. *Br J Radiol.* 2021;94(1118):20200854.
3. Ajmal M KM, Van Fossen K. . Breast Fibroadenoma StatPearls [Internet]. Treasure Island (FL): StatPearls Publishing; [updated 2022 Oct 6 2025 Jan. Available from: <https://www.ncbi.nlm.nih.gov/books/NBK535345/>.
4. Commission E. Final Report Summary - MAMMOCARE (Breast biopsy system guided by Positron Emission Mammography allowing real-time 3D visualization of tumour lesion and needle insertion guidance for higher sampling accuracy and efficiency) CORDIS2016 [Available from: <https://cordis.europa.eu/project/id/606017/reporting>.
5. Alipour S, Abedi M, Saberi A, Maleki-Hajiagha A, Faiz F, Shahsavari S, et al. Metformin as a new option in the medical management of breast fibroadenoma; a randomized clinical trial. *BMC Endocr Disord.* 2021;21(1):169.
6. Golatta M, Harcos A, Pavlista D, Danes J, Klein R, Simovich P, et al. Ultrasound-guided cryoablation of breast fibroadenoma: a pilot trial. *Arch Gynecol Obstet.* 2015;291(6):1355-60.
7. Klinger K, Bhimani C, Shames J, Sevrukov A. Fibroadenoma: From Imaging Evaluation to Treatment. 2019.
8. Pandit P, Murkey SP, Agarwal A, Jaiswal A, Agrawal S. Understanding Fibroadenoma of the Breast: A Comprehensive Review of Pre-operative and Post-operative Clinicopathological Correlations. *Cureus.* 2023;15(12):e51329.
9. Surgeons TAsOB. The Use of Transcutaneous and Percutaneous Ablation for the Treatment of Benign and Malignant Tumors of the Breast. 2018.
10. Forrai G, Kovács E, Ambrózay É, Barta M, Borbély K, Lengyel Z, et al. Use of Diagnostic Imaging Modalities in Modern Screening, Diagnostics and Management of Breast Tumours 1st Central-Eastern European Professional Consensus Statement on Breast Cancer. *Pathol Oncol Res.* 2022;28:1610382.
11. Graña-López L, Abelairas-López L, Villares A. Cryoablation in breast tumours. *Radiologia (Engl Ed).* 2025;67(2):214-22.
12. Rau AC, Siskey R, Ochoa JA, Good T. Factors Affecting Lethal Isotherms During Cryoablation Procedures. *Open Biomed Eng J.* 2016;10:62-71.
13. Ward RC, Lourenco AP, Mainiero MB. Ultrasound-Guided Breast Cancer Cryoablation. *AJR Am J Roentgenol.* 2019;213(3):716-22.
14. Hahn M, Pavlista D, Danes J, Klein R, Golatta M, Harcos A, et al. Ultrasound guided cryoablation of fibroadenomas. *Ultraschall Med.* 2013;34(1):64-8.
15. Sheth M, Lodhi U, Chen B, Park Y, McElligott S. Initial Institutional Experience With Cryoablation Therapy for Breast Fibroadenomas: Technique, Molecular Science, and Post-Therapy Imaging Follow-up. *J Ultrasound Med.* 2019;38(10):2769-76.
16. Early H, Aguilera J, Cheang E, McGahan J. Challenges and Considerations When Using Shear Wave Elastography to Evaluate the Transplanted Kidney, With Pictorial Review. *J Ultrasound Med.* 2017;36(9):1771-82.
17. Nankivell BJ, Borrowers RJ, Fung CL, O'Connell PJ, Allen RD, Chapman JR. The natural history of chronic allograft nephropathy. *N Engl J Med.* 2003;349(24):2326-33.

18. Solez K, Colvin RB, Racusen LC, Sis B, Halloran PF, Birk PE, et al. Banff '05 Meeting Report: differential diagnosis of chronic allograft injury and elimination of chronic allograft nephropathy ('CAN'). *Am J Transplant*. 2007;7(3):518-26.
19. Williams WW, Taheri D, Tolkoff-Rubin N, Colvin RB. Clinical role of the renal transplant biopsy. *Nat Rev Nephrol*. 2012;8(2):110-21.
20. Ahmad I. Biopsy of the transplanted kidney. *Semin Intervent Radiol*. 2004;21(4):275-81.
21. Furness PN, Philpott CM, Chorbajian MT, Nicholson ML, Bosmans JL, Corthouts BL, et al. Protocol biopsy of the stable renal transplant: a multicenter study of methods and complication rates. *Transplantation*. 2003;76(6):969-73.
22. Preda A, Van Dijk LC, Van Oostaijen JA, Pattynama PM. Complication rate and diagnostic yield of 515 consecutive ultrasound-guided biopsies of renal allografts and native kidneys using a 14-gauge Biopty gun. *Eur Radiol*. 2003;13(3):527-30.
23. Schwarz A, Gwinner W, Hiss M, Radermacher J, Mengel M, Haller H. Safety and adequacy of renal transplant protocol biopsies. *Am J Transplant*. 2005;5(8):1992-6.
24. Soudmand A, Ulu Ozturk F, Uslu N, Haberal N, Boyvat F, Moray G, et al. Efficacy of the Sonoelastography Method for Diagnosis of Fibrosis in Renal Transplant Patients. *Experimental and clinical transplantation : official journal of the Middle East Society for Organ Transplantation*. 2018.
25. Wilkinson A. Protocol transplant biopsies: are they really needed? *Clin J Am Soc Nephrol*. 2006;1(1):130-7.
26. Taljanovic MS, Gimber LH, Becker GW, Latt LD, Klauser AS, Melville DM, et al. Shear-Wave Elastography: Basic Physics and Musculoskeletal Applications. *Radiographics*. 2017;37(3):855-70.
27. Ophir J, Céspedes I, Ponnekanti H, Yazdi Y, Li X. Elastography: a quantitative method for imaging the elasticity of biological tissues. *Ultrason Imaging*. 1991;13(2):111-34.
28. Sigrist RMS, Liau J, Kaffas AE, Chammas MC, Willmann JK. Ultrasound Elastography: Review of Techniques and Clinical Applications. *Theranostics*. 2017;7(5):1303-29.
29. Chhajaj G, Arunachalam VK, Ramasamy R, Mehta P, Cherian M. Elastography: A surrogate marker of renal allograft fibrosis-quantification by shear-wave technique. *Polish Journal of Radiology*. 2021;86(1):e151-e6.
30. Lee J, Oh YT, Joo DJ, Ma BG, Lee AL, Lee JG, et al. Acoustic Radiation Force Impulse Measurement in Renal Transplantation: A Prospective, Longitudinal Study With Protocol Biopsies. *Medicine (Baltimore)*. 2015;94(39):e1590.
31. Syversveen T, Brabrand K, Midtvedt K, Strom EH, Hartmann A, Jakobsen JA, et al. Assessment of renal allograft fibrosis by acoustic radiation force impulse quantification--a pilot study. *Transpl Int*. 2011;24(1):100-5.
32. IceCure Medical. User manuals [Available from: <https://www.icecure-medical.com/products/user-manuals/>].
33. Cumpston M, Li T, Page MJ, Chandler J, Welch VA, Higgins JP, et al. Updated guidance for trusted systematic reviews: a new edition of the Cochrane Handbook for Systematic Reviews of Interventions. *Cochrane Database Syst Rev*. 2019;10:ED000142.
34. Whiting PF, Rutjes AW, Westwood ME, Mallett S, Deeks JJ, Reitsma JB, et al. QUADAS-2: a revised tool for the quality assessment of diagnostic accuracy studies. *Ann Intern Med*. 2011;155(8):529-36.
35. Guido Schwarzer JRC, Gerta Rücker. *Meta-Analysis with R*: Springer; 2015.

36. DerSimonian R, Laird N. Meta-analysis in clinical trials. *Control Clin Trials*. 1986;7(3):177-88.
37. Rödel E. Fisher, R. A.: *Statistical Methods for Research Workers*, 14. Aufl., Oliver & Boyd, Edinburgh, London 1970. XIII, 362 S., 12 Abb., 74 Tab., 40 s. *Biometrische Zeitschrift*. 1971;13(6):429-30.
38. Schober P, Boer C, Schwarte LA. Correlation Coefficients: Appropriate Use and Interpretation. *Anesth Analg*. 2018;126(5):1763-8.
39. Higgins JPT, Thompson SG, Deeks JJ, Altman DG. Measuring inconsistency in meta-analyses. *BMJ*. 2003;327(7414):557.
40. van Aert RCM, Schmid CH, Svensson D, Jackson D. Study specific prediction intervals for random-effects meta-analysis: A tutorial: Prediction intervals in meta-analysis. *Res Synth Methods*. 2021;12(4):429-47.
41. Agrawal D, Murthy N, Sanjeeva Shetty M, Hiremath D. Shear wave elastography in transplant kidney and its correlation with renal doppler parameters and eGFR. *International Journal of Radiology and Diagnostic Imaging*. 2021;4:86-91.
42. Barsoum NR, Elsisy AE, Mohamed MF, Hassan AA. Role of shear wave elastography in assessment of chronic allograft nephropathy. *Egyptian Journal of Radiology and Nuclear Medicine*. 2022;53(1).
43. Chiocchini ALC, Sportoletti C, Comai G, Brocchi S, Capelli I, Baraldi O, et al. Correlation Between Renal Cortical Stiffness and Histological Determinants by Point Shear-Wave Elastography in Patients With Kidney Transplantation. *Progress in transplantation (Aliso Viejo, Calif)*. 2017;27(4):346-53.
44. Dai X, Liu M, Guo Y, Zhao B, Tan Y, Xiang F. Noninvasive evaluation of renal allograft fibrosis by virtual touch tissues quantification. *Zhong nan da xue xue bao Yi xue ban = Journal of Central South University Medical sciences*. 2014;39(2):173-7.
45. Desvignes C, Dabadie A, Aschero A, Ruocco A, Garaix F, Daniel L, et al. Technical feasibility and correlations between shear-wave elastography and histology in kidney fibrosis in children. *Pediatric Radiology*. 2021;51(10):1879-88.
46. Ghonge NP, Mohan M, Kashyap V, Jasuja S. Renal allograft dysfunction: Evaluation with shear-wave sonoelastography. *Radiology*. 2018;288(1):146-52.
47. Grenier N, Poulain S, Lepreux S, Gennisson JL, Dallaudière B, Lebras Y, et al. Quantitative elastography of renal transplants using supersonic shear imaging: A pilot study. *European Radiology*. 2012;22(10):2138-46.
48. He WY, Jin YJ, Wang WP, Li CL, Ji ZB, Yang C. Tissue elasticity quantification by acoustic radiation force impulse for the assessment of renal allograft function. *Ultrasound in Medicine and Biology*. 2014;40(2):322-9.
49. Järv L, Kull I, Riispere Z, Kuudeberg A, Lember M, Ots-Rosenberg M. Ultrasound elastography correlations between anthropometrical parameters in kidney transplant recipients. *Journal of Investigative Medicine*. 2019;67(8):1137-41.
50. Qin C, Jin H, Zhang H, Zhang Y, Guan Z, Gao Y. Noninvasive Assessment of Interstitial Fibrosis and Tubular Atrophy in Renal Transplant by Combining Point-Shear Wave Elastography and Estimated Glomerular Filtration Rate. *Diagnostics (Basel)*. 2021;12(1).
51. Stock KF, Klein BS, Vo Cong MT, Sarkar O, Römisch M, Regenbogen C, et al. ARFI-based tissue elasticity quantification in comparison to histology for the diagnosis of renal transplant fibrosis. *Clinical Hemorheology and Microcirculation*. 2010;46(2-3):139-48.

52. Tukhbatullin MG, Galeev SR, Garifullina LI, Galeev RH. Shear wave ultrasound elastography to evaluate the state of renal transplant. *Sovremennye Tehnologii v Medicine*. 2017;9(4):131-5.
53. Wang HK, Lai YC, Lin YH, Chiou HJ, Chou YH. Acoustic Radiation Force Impulse Imaging of the Transplant Kidney: Correlation Between Cortical Stiffness and Arterial Resistance in Early Post-transplant Period. *Transplantation Proceedings*. 2017;49(5):1001-4.
54. Yang S, Liu Y, Zuo H, Feng L, Xu C, Gu L, et al. Effects of body parameters on renal cortical stiffness measured by shear-wave elastography in patients with kidney transplantation. *Zhong Nan Da Xue Xue Bao Yi Xue Ban*. 2022;47(10):1385-91.
55. Page MJ, McKenzie JE, Bossuyt PM, Boutron I, Hoffmann TC, Mulrow CD, et al. The PRISMA 2020 statement: An updated guideline for reporting systematic reviews. *J Clin Epidemiol*. 2021;134:178-89.
56. Carriero S, Depretto C, Cozzi A, Della Pepa G, D'Ascoli E, Irmici G, et al. Efficacy and safety of vacuum-assisted excision (VAE) of fibroadenomas: experience in a tertiary centre. *Radiol Med*. 2023;128(10):1199-205.
57. Fine RE, Whitworth PW, Kim JA, Harness JK, Boyd BA, Burak WE, Jr. Low-risk palpable breast masses removed using a vacuum-assisted hand-held device. *Am J Surg*. 2003;186(4):362-7.
58. Ward RC, Wang Y, Lourenco AP, Mainiero MB. Symptomatic Fibroadenoma Resolves Status Post Cryoablation. *R I Med J* (2013). 2019;102(8):49-52.
59. Challapalli JV, Yoon JH, Ward RC. Breast Cryoablation, From the AJR "How We Do It" Special Series. *AJR Am J Roentgenol*. 2025;224(3):e2431025.
60. Díaz de Bustamante Durbán T, Roca Navarro MJ, Navarro Monforte Y, Garrido Alonso D, García Martínez F, Córdoba Chicote MV, et al. Ultrasound-guided cryoablation: Our experience in percutaneous treatment as an alternative to surgery for fibroadenomas of the breast lesions. *Radiologia (Engl Ed)*. 2024;66(3):228-35.
61. Vyas KP, Cannavo MD, Ward RC. Breast Cryoablation: Techniques, Indications, and Challenges. *Current Radiology Reports*. 2023;11(4):60-8.
62. Fine RE, Gilmore RC, Tomkovich KR, Dietz JR, Berry MP, Hernandez LE, et al. Cryoablation Without Excision for Early-Stage Breast Cancer: ICE3 Trial 5-Year Follow-Up on Ipsilateral Breast Tumor Recurrence. *Ann Surg Oncol*. 2024;31(11):7273-83.
63. Habrawi Z, Melkus MW, Khan S, Henderson J, Brandi L, Chu V, et al. Cryoablation: A promising non-operative therapy for low-risk breast cancer. *Am J Surg*. 2021;221(1):127-33.
64. van de Voort EMF, Klem T, Struik GM, Birnie E, Sinke R, Ghandi A. Patient reported cosmetic outcome after vacuum assisted excision of benign breast lesions: a cross-sectional study. *Br J Radiol*. 2020;93(1114):20190994.
65. Kawamoto H, Tsugawa K, Furuya Y, Sakamaki K, Kakimoto S, Kitajima M, et al. Percutaneous ultrasound-guided cryoablation for early-stage primary breast cancer: a follow-up study in Japan. *Breast Cancer*. 2024;31(4):695-704.
66. Holmes D, Iyengar G. Breast Cancer Cryoablation in the Multidisciplinary Setting: Practical Guidelines for Patients and Physicians. *Life (Basel)*. 2023;13(8).
67. Cassinotto C, Boursier J, de Ledinghen V, Lebigot J, Lapuyade B, Cales P, et al. Liver stiffness in nonalcoholic fatty liver disease: A comparison of supersonic shear imaging, FibroScan, and ARFI with liver biopsy. *Hepatology*. 2016;63(6):1817-27.
68. Friedrich-Rust M, Lupsor M, de Knegt R, Dries V, Buggisch P, Gebel M, et al. Point Shear Wave Elastography by Acoustic Radiation Force Impulse Quantification in

Comparison to Transient Elastography for the Noninvasive Assessment of Liver Fibrosis in Chronic Hepatitis C: A Prospective International Multicenter Study. *Ultraschall Med.* 2015;36(3):239-47.

69. Sporea I, Sirli R, Bota S, Fierbinteanu-Braticevici C, Petrisor A, Badea R, et al. Is ARFI elastography reliable for predicting fibrosis severity in chronic HCV hepatitis? *World J Radiol.* 2011;3(7):188-93.

70. Ye XP, Ran HT, Cheng J, Zhu YF, Zhang DZ, Zhang P, et al. Liver and spleen stiffness measured by acoustic radiation force impulse elastography for noninvasive assessment of liver fibrosis and esophageal varices in patients with chronic hepatitis B. *J Ultrasound Med.* 2012;31(8):1245-53.

71. Zhuang Y, Ding H, Zhang Y, Sun H, Xu C, Wang W. Two-dimensional Shear-Wave Elastography Performance in the Noninvasive Evaluation of Liver Fibrosis in Patients with Chronic Hepatitis B: Comparison with Serum Fibrosis Indexes. *Radiology.* 2017;283(3):873-82.

72. Grenier N, Gennisson JL, Cornelis F, Le Bras Y, Couzi L. Renal ultrasound elastography. *Diagn Interv Imaging.* 2013;94(5):545-50.

73. Lee CU, Glockner JF, Glaser KJ, Yin M, Chen J, Kawashima A, et al. MR elastography in renal transplant patients and correlation with renal allograft biopsy: a feasibility study. *Acad Radiol.* 2012;19(7):834-41.

74. Low G, Kruse SA, Lomas DJ. General review of magnetic resonance elastography. *World J Radiol.* 2016;8(1):59-72.

75. Marticorena Garcia SR, Fischer T, Dürr M, Gültekin E, Braun J, Sack I, et al. Multifrequency Magnetic Resonance Elastography for the Assessment of Renal Allograft Function. *Invest Radiol.* 2016;51(9):591-5.

76. Kirpalani A, Hashim E, Leung G, Kim JK, Krizova A, Jothy S, et al. Magnetic Resonance Elastography to Assess Fibrosis in Kidney Allografts. *Clin J Am Soc Nephrol.* 2017;12(10):1671-9.

77. Naesens M, Kuypers DR, De Vusser K, Evenepoel P, Claes K, Bammens B, et al. The histology of kidney transplant failure: a long-term follow-up study. *Transplantation.* 2014;98(4):427-35.

78. Seron D, Arns W, Chapman JR. Chronic allograft nephropathy--clinical guidance for early detection and early intervention strategies. *Nephrol Dial Transplant.* 2008;23(8):2467-73.

79. Racusen LC, Solez K, Colvin RB, Bonsib SM, Castro MC, Cavallo T, et al. The Banff 97 working classification of renal allograft pathology. *Kidney Int.* 1999;55(2):713-23.

80. Roufosse C, Simmonds N, Clahsen-van Groningen M, Haas M, Henriksen KJ, Horsfield C, et al. A 2018 Reference Guide to the Banff Classification of Renal Allograft Pathology. *Transplantation.* 2018;102(11):1795-814.

81. Akgul A, Ibis A, Sezer S, Basaran C, Usluogullari A, Ozdemir FN, et al. Early assessment of renal resistance index and long-term renal function in renal transplant recipients. *Ren Fail.* 2009;31(1):18-24.

82. Goncalves LM, Forte GC, Holz TG, Libermann LL, de Figueiredo CEP, Hochegger B. Shear wave elastography and Doppler ultrasound in kidney transplant recipients. *Radiol Bras.* 2022;55(1):19-23.

83. Ikee R, Kobayashi S, Hemmi N, Imakiire T, Kikuchi Y, Moriya H, et al. Correlation between the resistive index by Doppler ultrasound and kidney function and histology. *Am J Kidney Dis.* 2005;46(4):603-9.

84. Kolonko A, Chudek J, Zejda JE, Wiecek A. Impact of early kidney resistance index on kidney graft and patient survival during a 5-year follow-up. *Nephrol Dial Transplant*. 2012;27(3):1225-31.
85. Looock MT, Bamoulid J, Courivaud C, Manzoni P, Simula-Faivre D, Chalopin JM, et al. Significant increase in 1-year posttransplant renal arterial index predicts graft loss. *Clin J Am Soc Nephrol*. 2010;5(10):1867-72.
86. Radermacher J, Mengel M, Ellis S, Stuht S, Hiss M, Schwarz A, et al. The renal arterial resistance index and renal allograft survival. *N Engl J Med*. 2003;349(2):115-24.
87. Spatola L, Andrulli S. Doppler ultrasound in kidney diseases: a key parameter in clinical long-term follow-up. *J Ultrasound*. 2016;19(4):243-50.
88. Urban MW, Rule AD, Atwell TD, Chen S. Novel Uses of Ultrasound to Assess Kidney Mechanical Properties. *Kidney360*. 2021;2(9):1531-9.
89. Chapman JR, O'Connell PJ, Nankivell BJ. Chronic renal allograft dysfunction. *J Am Soc Nephrol*. 2005;16(10):3015-26.
90. Wang J, Yan J, Zhang T, Cai H, Yang W, Ying L, et al. Predicting Adverse Outcomes in Kidney Transplant Recipients Using an Interpretable Model Based on Shear-Wave Elastography. *Kidney Dis (Basel)*. 2025;11(1):469-81.
91. Ruidas S, Lal H, Prasad R, Sharma S, Agarwal S, Singh R, et al. Role of Shear Wave Elastography for Assessment of Renal-Allograft Fibrosis and its Correlation With Histopathology. *J Ultrasound Med*. 2024;43(10):1979-92.
92. Zhang TY, Yan J, Wu J, Yang W, Zhang S, Xia J, et al. Shear wave elastography parameters adds prognostic value to adverse outcome in kidney transplantation recipients. *Ren Fail*. 2023;45(1):2235015.
93. Chen A, Wang Y, Yang Y, Luo S, Chen X, Zhou J. Application of ultrasonography elastography in chronic transplanted kidney renal insufficiency: a narrative review. *Quant Imaging Med Surg*. 2025;15(10):10262-79.
94. Ferraioli G, Barr RG, Berzigotti A, Sporea I, Wong VW, Reiberger T, et al. WFUMB Guideline/Guidance on Liver Multiparametric Ultrasound: Part 1. Update to 2018 Guidelines on Liver Ultrasound Elastography. *Ultrasound Med Biol*. 2024;50(8):1071-87.
95. Charoenchue P, Khorana J, Chitapanarux T, Inmutto N, Na Chiangmai W, Amantakul A, et al. Two-Dimensional Shear-Wave Elastography: Accuracy in Liver Fibrosis Staging Using Magnetic Resonance Elastography as the Reference Standard. *Diagnostics (Basel)*. 2024;15(1).
96. Maingard J, Kok HK, Ranatunga D, Brooks DM, Chandra RV, Lee MJ, et al. The future of interventional and neurointerventional radiology: learning lessons from the past. *Br J Radiol*. 2017;90(1080):20170473.
97. Tilney NL. Renal transplantation. *Curr Probl Surg*. 1989;26(9):601-69.

16. BIBLIOGRAPHY

16.1. Publications Related to the Thesis

Cryoablation for Fibroadenoma with Liquid Nitrogen Based System: a retrospective analysis of prospectively collected data

Filipov Teodóra, Teutsch Brigitta, Dorina Vass, Boglárka Budinszki, Péter Hegyi, Attila Doros, Gábor Forrai, Pál Ákos Deák

PLOS ONE (2025)

DOI: 10.1371/journal.pone.0340969

Q1 JIF: 2.3

Investigating the role of ultrasound-based shear wave elastography in kidney transplanted patients : correlation between non-invasive fibrosis detection, kidney dysfunction and biopsy results-a systematic review and meta-analysis

Filipov Teodóra, Teutsch Brigitta, Szabó Anett, Forintos Attila, Ács Júlia, Váradi Alex, Hegyi Péter, Szarvas Tibor, Ács Nándor, Nyirády Péter, Deák Pál Ákos

JOURNAL OF NEPHROLOGY (2024)

DOI: 10.1007/s40620-023-01856-w

Q1 JIF: 2.6

16.2. Publications not Related to the Thesis

Lifestyle-, environmental-, and additional health factors associated with an increased sperm DNA fragmentation : a systematic review and meta-analysis

Szabó Anett, Váncsa Szilárd, Hegyi Péter, Váradi Alex, Forintos Attila, **Filipov Teodóra**, Ács Júlia, Ács Nándor, Szarvas Tibor, Nyirády Péter, Kopa Zsolt

REPRODUCTIVE BIOLOGY AND ENDOCRINOLOGY (2023)

DOI: 10.1186/s12958-023-01054-0

D1 JIF: 4.6

17. ACKNOWLEDGEMENTS

I am deeply grateful to the many people who have supported and accompanied me throughout this journey.

First, I would like to express my sincere gratitude to my supervisor Ákos, whose belief in me never wavered. Your constant support, trust, and patience were invaluable, and I am deeply thankful that you never lost faith in me, even during challenging moments.

I would also like to wholeheartedly thank Brigi and Szilárd for being exceptional scientific methodology supervisors. Your guidance, encouragement, and gentle nudging in the right direction were invaluable to this work.

My heartfelt thanks go to my dear friends Marci and Gigi, for their support and insightful advice. Your clarity, dedication, and encouragement played a crucial role in the completion of this thesis, and without you, this work would not have been possible.

I am immensely grateful to all my amazing friends, who continuously pushed me forward, lifted me up, and were always there to catch me when I stumbled. Your encouragement, laughter, and belief in me have been fundamental in shaping who I am today.

To my family, thank you for your eternal support and unconditional love. Knowing you were always there gave me the strength to persevere.

Finally, I thank the entire CTM team and all collaborators for making this journey possible. Your support and collaboration created an environment in which this work could truly come to life.